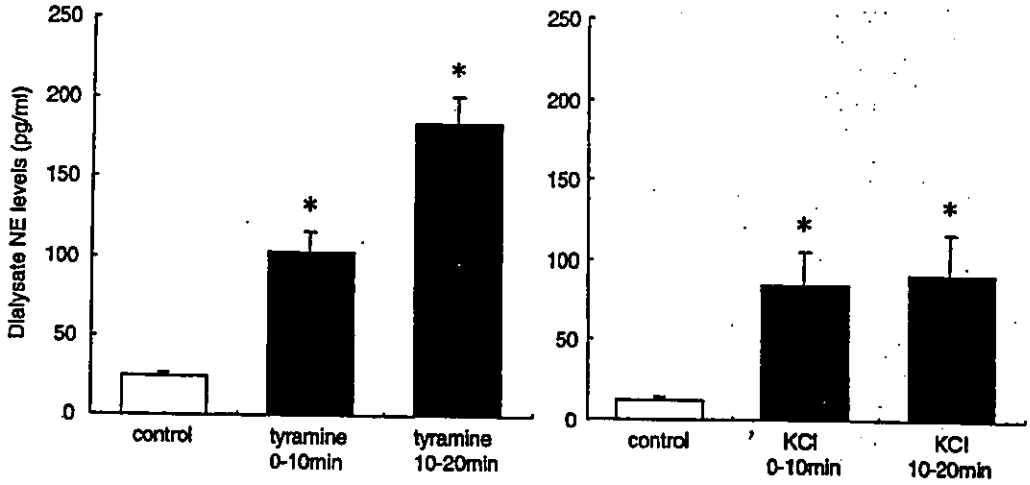

Fig. 3. Local administration of tyramine (600 μM ($n = 6$)) and KCl (100 mM ($n = 5$)) markedly increased the dialysate NE levels. NE: norepinephrine. *$P < 0.05$ vs. control.

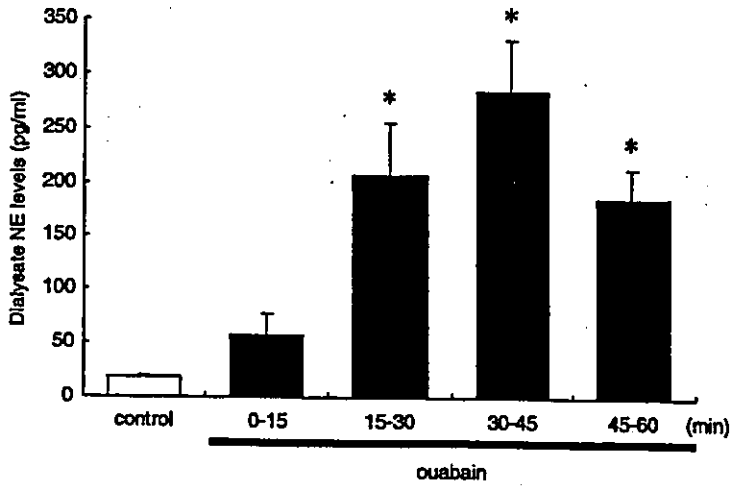

Fig. 4. Time course of the dialysate NE levels during ouabain (100 μM) administration ($n = 6$). NE: norepinephrine. *$P < 0.05$ vs. control.

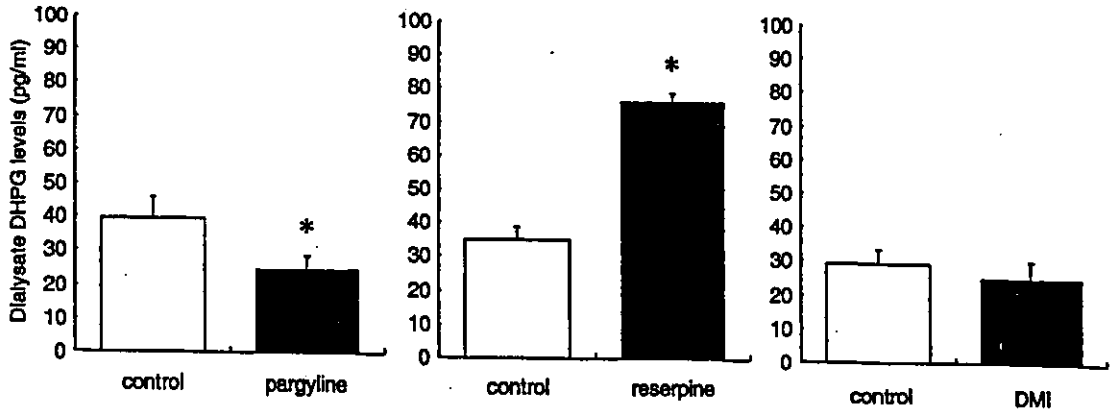

Fig. 5. Local administration of pargyline (1 mM) decreased dialysate DHPG levels ($n = 7$). Reserpine (10 μM) increased dialysate DHPG levels ($n = 5$). DHPG: dihydroxyphenylglycol; DMI: desipramine. *$P < 0.05$ vs. control.

Table 1
Comparison of dialysate NE and its metabolites between cardiac and skeletal muscle

	Cardiac muscle	Skeletal muscle
NE (pg/ml)	57.3 ± 13.7	11.7 ± 1.2
DHPG (pg/ml)	353.1 ± 53.4	38.1 ± 3.2
MHPG (pg/ml)	447.3 ± 64.3	266.1 ± 28.7

NE: norepinephrine; DHPG: dihydroxyphenylglycol; MHPG: 3-methoxy-4-hydroxyphenylglycol.

DHPG, and MHPG levels averaged 11.7 ± 1.2, 38.1 ± 3.2, and 266.1 ± 28.7 pg/ml, respectively.

4. Discussion

At the skeletal muscle, the small amount of dialysate NE and its metabolites could be determined by the microdialysis coupling with electrochemical detection. The levels of interstitial NE and its metabolites might be affected by circulating NE and surrounding sympathetic tissue. Local administration of TTX markedly decreased dialysate NE. Our data suggest that the reduction of dialysate NE was derived from surrounding sympathetic nerve and remaining amount of NE was derived from circulating NE. Furthermore, desipramine increased dialysate NE. These results suggest that basal NE levels in dialysate were regulated by depolarization-induced exocytotic NE release and NE uptake. Therefore, function of surrounding sympathetic nerve endings was responsible for the basal dialysate NE level. This result is consistent with an early study in which the plasma NE level in vein draining skeletal muscle was noted to be higher than the arterial plasma level, indicating regional production of NE from sympathetic nerve endings (Esler et al., 1987). The dialysate DHPG levels were also altered by local administration of pargyline and reserpine which affected intraneuronal compartments. Both dialysate NE and its metabolite were derived mainly from surrounding sympathetic nerve endings. Thus, skeletal muscle NE and its metabolites reflect information about regional NE kinetics.

Data on NE spillover suggested that as much as 20–30% of the NE entering the circulation derived from skeletal muscle sympathetic nerves (Esler et al., 1984). Therefore, it is important to determine the function of NE release from skeletal muscle sympathetic nerves. Assessment of NE release from sympathetic nerve endings was performed with local administration of high K^+ and ouabain through the dialysis probe. Both high K^+ and ouabain induced increases in dialysate NE levels. On the other hand, cardiac NE spillover accounts for 2–3% of total body NE release to plasma (Esler et al., 1984), and high K^+ and ouabain-induced NE responses were five-fold higher than those of skeletal muscle (Yamazaki et al., 1998, 1999). In contrast to a dense innervated cardiac sympathetic nerve, the skeletal muscle has a thin sympathetic innervation, but organ mass or blood flow contributes to a large amount of NE spillover from the skeletal muscle. Thus, little increments in NE release at the skeletal muscle sympathetic nerve may affect circulating plasma NE levels.

In experimental or clinical conditions, sympathetic nerve innervation was determined pharmacologically by responsiveness to tyramine (Shannon et al., 2000; Takauchi et al., 2000). In in situ innervated skeletal muscle, local administration of tyramine caused a brisk increase in dialysate NE levels. High K^+ and tyramine induced increments in dialysate NE. These drugs act with different NE releasing mechanisms (Nicholls, 1994). Local administration of tyramine acted by releasing NE from stored vesicle with membrane and vesicle NE transporters (Langeloh et al., 1987; Trendelenburg et al., 1987). The level of dialysate NE evoked by tyramine seems to reflect the total NE content at the nerve endings. Therefore, the dialysate response could examine whether sympathetic nerve endings preserve vesicle NE content, membrane and vesicle NE transporters.

Data on experimental hypertension in rats demonstrated that NE uptake is impaired in skeletal muscle (Cabassi et al., 2001). Reduced NE uptake may be responsible for pathogenesis of hypertension. Microdialysis with local administration of pharmacological agents is particularly appropriate to identify impairment of regional NE uptake function (Yamazaki et al., 1997). Neuronal NE uptake function was assessed by local administration of desipramine. Desipramine induced an increment in dialysate NE but did not affect dialysate DHPG levels. Desipramine induced a two-fold increase in dialysate NE. Early studies indicate that this ratio is independent of NE release, but instead dependent on NE uptake function (Yamazaki and Akiyama, 1996; Yamazaki et al., 1997). Therefore, a comparison of the dialysate NE level between the presence and absence of desipramine reveals that neuronal NE uptake, to a variable extent, is involved in dialysate NE changes.

DHPG is a deaminated metabolite of NE (Kopin, 1985). Previous studies in cardiac microdialysis reported that, in the presence of an intact MAO system, DHPG serves as an index of the cytosolic (axoplasmic) NE level (Yamazaki et al., 1997, 2001a). Basal DHPG levels were altered by local administration of reserpine, but not by desipramine. These data suggested that basal dialysate DHPG level corresponds to vesicle NE mobilization rather than membrane NE uptake. Therefore these data support the conclusion that the production of DHPG is mainly due to intraneuronal MAO at surrounding skeletal muscle sympathetic nerve endings and that measurement of dialysate DHPG provides information about organ-specific vesicular uptake function rather than membrane NE uptake.

Basal dialysate MHPG level was higher than basal DHPG level. MHPG is also a major metabolite of NE. MHPG is produced by extraneuronal *O*-methylation of DHPG formed intraneuronally from NE or by the extraneuronal combination of COMT and MAO on NE (Kopin, 1985). Higher MHPG levels may suggest activity of extraneuronal NE degradation in physiological conditions. In fact, Lambert et al. described that the majority of MHPG in plasma is

derived from skeletal muscle (Lambert et al., 1995). Our data suggested that alteration of intraneuronal NE metabolism did not affect dialysate MHPG levels. Acute reflex stimulation of sympathetic nerve activity was not associated with parallel changes in regional MHPG production (Lambert et al., 1995). Further studies concerning the role of MHPG on skeletal muscle NE kinetics are warranted.

4.1. Methodological consideration

Several limitations and problems cast doubt on the validity of microdialysis technique as an index of regional sympathetic nerve function. The first limitation is related to the fact that we investigated the skeletal muscle NE and its metabolites in rabbits anesthetized with pentobarbital sodium. The anesthesia affects both the afferent and efferent sympathetic nerve tracts, and so may modify the NE response (Zimpfer et al., 1982). We agree with the influence of anesthesia on the autonomic control. Our final goal of these experiments is to investigate the skeletal muscle NE kinetics in conscious animals and clinical fields. Further studies concerning non-anesthetized animals and humans are warranted.

The second problem is related to the origin and physiological implication of sympathetic nerve endings in skeletal muscle. At the skeletal muscle, sympathetic nerve endings are histochemically located in blood vessels, muscle spindle, and skeletal muscle fibers (Barker and Saito, 1981). However, it is uncertain whether the obtained NE is derived mainly from specific sites and in what proportion. Furthermore, the sympathetic system can influence skeletal muscle contraction (Grassi and Passatore, 1988, 1990), blood flow (Lundvall and Edfeldt, 1994; Thompson and Mohrman, 1983), and glucose metabolism (Fagius and Berne, 1994; Spraul et al., 1994). The functional implications of NE release are an important focus for future studies.

Dialysis technique was used to determine interstitial NE and its metabolites in the heart and skeletal muscle. Basal NE level in the heart was five-fold higher than that of the skeletal muscle. Cardiac DHPG level was nine-fold higher than that of skeletal muscle. MHPG level in the heart was slightly higher than that of skeletal muscle. These studies show that intraneuronal NE turnover was more active in the heart, but in the skeletal muscle intraneronal NE turnover was less active and extraneuornal NE degradation was more active. Eisenhofer suggested that most released NE was captured by the NE uptake system, whereas extracted NE through the circulating NE might be captured by the extraneuronal NE uptake system (Eisenhofer, 2001). Dispersed organ systems, such as skeletal muscle, have a thin and diffuse sympathetic innervation, but being a large organ mass, the skeletal muscle NE and its metabolites cannot be ignored.

Acknowledgements

This work was supported by Grants-in-Aid for scientific research (13470154, 13877114) from the Ministry of Education, Culture, Sports, Science and Technology; New Energy and Industrial Technology Development Organization; the Research Grants for Cardiovascular Disease (H13C-1) from the Ministry of Health, Labor and Welfare; the Promotion Fundamental Studies in Health Science of the Organization for Pharmaceutical Safety and Research of Japan.

References

Akiyama, T., Yamazaki, T., Ninomiya, I., 1991. In vivo monitoring of myocardial interstitial norepinephrine by dialysis technique. Am. J. Physiol. 261, H1643–H1647.

Anderson, E.A., Sinkey, C.A., Lawton, W.J., Mark, A.L., 1989. Elevated sympathetic nerve activity in borderline hypertensive humans. Evidence from direct intraneural recordings. Hypertension 14, 177–183.

Aneman, A., Eisenhofer, G., Olbe, L., Dalenback, J., Nitescu, P., Fandriks, L., Friberg, P., 1996. Sympathetic discharge to mesenteric organs and the liver. Evidence for substantial mesenteric organ norepinephrine spillover. J. Clin. Invest. 97, 1640–1646.

Anton, A.H., Sayer, D.F., 1962. A study of the factors affecting the aluminum oxide-trihydroxyindole procedure for the analysis of catecholamine. J. Pharmacol. Exp. Ther. 138, 360–375.

Arner, P., Bolinder, J., Eliasson, A., 1988. Microdialysis of adipose tissue and blood for in vivo lipolysis studies. Am. J. Physiol. 255, E737–E742.

Barker, D., Saito, M., 1981. Autonomic innervation of receptors and muscle fibres in cat skeletal muscle. Proc. R. Soc. Lond. B: Biol. Sci. 212, 317–332.

Bruce, S., Tack, C., Patel, J., Pacak, K., Goldstein, D.S., 2002. Local sympathetic function in human skeletal muscle and adipose tissue assessed by microdialysis. Clin. Auton. Res. 12, 13–19.

Cabassi, A., Vinci, S., Quartieri, F., Moschini, L., Borghetti, A., 2001. Norepinephrine reuptake is impaired in skeletal muscle of hypertensive rats in vivo. Hypertension 37, 698–702.

Eisenhofer, G., 2001. The role of neuronal and extraneuronal plasma membrane transporters in the inactivation of peripheral catecholamines. Pharmacol. Ther. 91, 35–62.

Esler, M., Jennings, G., Leonard, P., Sacharias, N., Burke, F., Johns, J., Blombery, P., 1984. Contribution of individual organs to total noradrenaline release in humans. Acta Physiol. Scand. Suppl. 527, 11–16.

Esler, M., Jennings, G., Lambert, G., Korner, P., 1987. Local autonomic activity in primary hypertension. In: Hofman, A., Grobee, D.E., Schalekamp, M.A.D.H. (Eds.), The Early Pathogenesis of Primary Hypertension. Excerpta Medica (International Congress Series 737), Amsterdam, pp. 141–155.

Fagius, J., Berne, C., 1994. Increase in muscle nerve sympathetic activity in humans after food intake. Clin. Sci. (London) 86, 159–167.

Ferguson, D.W., Berg, W.J., Sanders, J.S., 1990. Clinical and hemodynamic correlates of sympathetic nerve activity in normal humans and patients with heart failure: evidence from direct microneurographic recordings. J. Am. Coll. Cardiol. 16, 1125–1134.

Grassi, C., Passatore, M., 1988. Action of the sympathetic system on skeletal muscle. Ital. J. Neurol. Sci. 9, 23–28.

Grassi, C., Passatore, M., 1990. Spontaneous sympathetic command to skeletal muscles: functional implications. Funct. Neurol. 5, 227–232.

Grassi, G., Seravalle, G., Cattaneo, B.M., Lanfranchi, A., Vailati, S., Giannattasio, C., Del Bo, A., Sala, C., Bolla, G.B., Pozzi, M., 1995. Sympathetic activation and loss of reflex sympathetic control in mild congestive heart failure. Circulation 92, 3206–3211.

Gronlund, B., Astrup, A., Bie, P., Christensen, N.J., 1991. Noradrenaline release in skeletal muscle and in adipose tissue studied by microdialysis. Clin. Sci. 80, 595–598.

Kiss, J.P., Zsilla, G., Mike, A., Zelles, T., Toth, E., Lajtha, A., Vizi, E.S., 1995. Subtype-specificity of the presynaptic alpha 2-adrenoceptors modulating hippocampal norepinephrine release in rat. Brain Res. 674, 238–244.

Kopin, I.J., 1985. Catecholamine metabolism: basic aspects and clinical significance. Pharmacol. Rev. 37, 333–364.

Lambert, G.W., Kaye, D.M., Vaz, M., Cox, H.S., Turner, A.G., Jennings, G.L., Esler, M.D., 1995. Regional origins of 3-methoxy-4-hydroxyphenylglycol in plasma: effects of chronic sympathetic nervous activation and denervation, and acute reflex sympathetic stimulation. J. Auton. Nerv. Syst. 55, 169–178.

Langeloh, A., Bonisch, H., Trendelenburg, U., 1987. The mechanism of the 3H-noradrenaline releasing effect of various substrates of uptake1: multifactorial induction of outward transport. Naunyn Schmiedebergs Arch. Pharmacol. 336, 602–610.

Lundvall, J., Edfeldt, H., 1994. Very large range of baroreflex sympathetic control of vascular resistance in human skeletal muscle and skin. J. Appl. Physiol. 76, 204–211.

Mundinger, T.O., Boyle, M.R., Taborsky Jr., G.J., 1997. Activation of hepatic sympathetic nerves during hypoxic, hypotensive and glucopenic stress. J. Auton. Nerv. Syst. 63, 153–160.

Nicholls, D.G., 1994. Proteins, Transmitters and Synapses. Blackwell Scientific Publications, Oxford, pp. 32–33.

Shannon, J.R., Flattem, N.L., Jordan, J., Jacob, G., Black, B.K., Biaggioni, I., Blakely, R.D., Robertson, D., 2000. Orthostatic intolerance and tachycardia associated with norepinephrine-transporter deficiency. N. Engl. J. Med. 342, 541–549.

Spraul, M., Anderson, E.A., Bogardus, C., Ravussin, E., 1994. Muscle sympathetic nerve activity in response to glucose ingestion. Impact of plasma insulin and body fat. Diabetes 43, 191–196.

Takauchi, Y., Kitagawa, H., Kawada, T., Akiyama, T., Yamazaki, T., 1997. High-performance liquid chromatographic determination of myocardial interstitial dihydroxyphenylglycol. J. Chromatogr. B: Biomed. Sci. Appl. 693, 218–221.

Takauchi, Y., Yamazaki, T., Akiyama, T., 2000. Tyramine-induced endogeneous noradrenaline efflux from in situ cardiac sympathetic nerve ending in cats. Acta Physiol. Scand. 168, 287–293.

Thompson, L.P., Mohrman, D.E., 1983. Blood flow and oxygen consumption in skeletal muscle during sympathetic stimulation. Am. J. Physiol. 245, H66–H71.

Thompson, J.M., Wallin, B.G., Lambert, G.W., Jennings, G.L., Esler, M.D., 1998. Human muscle sympathetic activity and cardiac catecholamine spillover: no support for augmented sympathetic noradrenaline release by adrenaline co-transmission. Clin. Sci. (London) 94, 383–393.

Trendelenburg, U., Langeloh, A., Bonisch, H., 1987. Mechanism of action of indirectly acting sympathomimetic amines. Blood Vessels 24, 261–270.

Wallin, B.G., Thompson, J.M., Jennings, G.L., Esler, M.D., 1996. Renal noradrenaline spillover correlates with muscle sympathetic activity in humans. J. Physiol. 491, 881–887.

Yamazaki, T., Akiyama, T., 1996. Effects of locally administered desipramine on myocardial interstitial norepinephrine levels. J. Auton. Nerv. Syst. 61, 264–268.

Yamazaki, T., Akiyama, T., Shindo, T., 1995. Routine high-performance liquid chromatographic determination of myocardial interstitial norepinephrine. J. Chromatogr. B: Biomed. Appl. 670, 328–331.

Yamazaki, T., Akiyama, T., Kitagawa, H., Takauchi, Y., Kawada, T., Sunagawa, K., 1997. A new, concise dialysis approach to assessment of cardiac sympathetic nerve terminal abnormalities. Am. J. Physiol. 272, H1182–H1187.

Yamazaki, T., Akiyama, T., Kawada, T., Kitagawa, H., Takauchi, Y., Yahagi, N., Sunagawa, K., 1998. Norepinephrine efflux evoked by potassium chloride in cat sympathetic nerves: dual mechanism of action. Brain Res. 794, 146–150.

Yamazaki, T., Akiyama, T., Kawada, T., 1999. Effects of ouabain on in situ cardiac sympathetic nerve endings. Neurochem. Int. 35, 439–445.

Yamazaki, T., Akiyama, T., Kitagawa, H., Kawada, T., Sunagawa, K., 2001a. Dialysate dihydroxyphenylglycol as a window for in situ axoplasmic norepinephrine disposition. Neurochem. Int. 38, 287–292.

Yamazaki, T., Akiyama, T., Mori, H., 2001b. Effects of nociceptin on cardiac norepinephrine and acetylcholine release evoked by ouabain. Brain Res. 904, 153–156.

Youdim, M.B.H., Finberg, J.P.M., Tipton, K.F., 1988. Monoamine oxidase. In: Trendelenburg, U., Weiner, N. (Eds.), Handbook of Experimental Pharmacology. Catecholamine 1, vol. 90/1. Springer, Berlin, pp. 119–192.

Zimpfer, M., Manders, W.T., Barger, A.C., Vatner, S.F., 1982. Pentobarbital alters compensatory neural and humoral mechanisms in response to hemorrhage. Am. J. Physiol. 243, H713–H721.

Zou, A.P., Cowley Jr., A.W., 1997. Nitric oxide in renal cortex and medulla. An in vivo microdialysis study. Hypertension 29, 194–198.

British Journal of Pharmacology (2003) 139, 899–910
www.nature.com/bjp

Changes in functional and histological distributions of nitric oxide synthase caused by chronic hypoxia in rat small pulmonary arteries

*,[1]Mikiyasu Shirai, [1]James T. Pearson, [1]Akito Shimouchi, [1]Noritoshi Nagaya, [1]Hirotsugu Tsuchimochi, [2]Ishio Ninomiya & [1]Hidezo Mori

[1]Department of Cardiac Physiology, National Cardiovascular Centre Research Institute, 5-7-1 Fujishiro-dai, Suita, Osaka 565-8565, Japan and [2]Department of Engineering, Faculty of Health Sciences, Hiroshima International University, Hiroshima 724-0695, Japan

1 Chronic hypoxia (CH) increases lung tissue expression of all types of nitric oxide synthase (NOS) in the rat. However, it remains unknown whether CH-induced changes in functional and histological NOS distributions are correlated in rat small pulmonary arteries.

2 We measured the effects of NOS inhibitors on the internal diameters (ID) of muscular (MPA) and elastic (EPA) pulmonary arteries (100–700 μm ID) using an X-ray television system on anaesthetized rats. We also conducted NOS immunohistochemical localization on the same vessels.

3 Nonselective NOS inhibitors induced ID reductions in almost all MPA of CH rats (mean reduction, 36±3%), as compared to ~60% of control rat MPA (mean, 10±2%). The inhibitors reduced the ID of almost all EPA with similar mean values (~26%) in both CH and control rats. On the other hand, inducible NOS (iNOS)-selective inhibitors caused ID reductions in ~60% of CH rat MPA (mean, 15±3%), but did so in only ~20% of control rat MPA (mean, 2±2%). This inhibition caused only a small reduction (mean, ~4%) in both CH and control rat EPA. A neuronal NOS-selective inhibitor had no effect.

4 The percentage of endothelial NOS (eNOS)-positive vessels was ~96% in both MPA and EPA from CH rats, whereas it was 51 and 91% in control MPA and EPA, respectively. The percentage for iNOS was ~60% in both MPA and EPA from CH rats, but was only ~8% in both arteries from control rats.

5 The data indicate that in CH rats, both functional and histological upregulation of eNOS extensively occurs within MPA. iNOS protein increases sporadically among parallel-arranged branches in both MPA and EPA, but its vasodilatory effect is predominantly observed in MPA. Such NOS upregulation may serve to attenuate hypoxic vasoconstriction, which occurs primarily in MPA and inhibit the progress of pulmonary hypertension.
British Journal of Pharmacology (2003) **139**, 899–910. doi:10.1038/sj.bjp.0705312

Keywords: Chronic hypoxia; pulmonary hypertension; small pulmonary arteries; endogenous NO; L-NAME; L-NMMA; L-canavanine; s-methylisothiourea; 7-nitro indazole; NOS immunohistochemistry

Abbreviations: CH, chronic hypoxia; GMP, guanosine-3′,5′-monophosphate; ID, internal diameter; LV, left ventricle; L-NAME, N^{ω}-nitro-L-arginine methyl ester; L-NMMA, N^{ω}-monomethyl-L-arginine; NO, nitric oxide; eNOS, endothelial NO synthase; iNOS, inducible NO synthase; nNOS, neuronal NO synthase; PAP, pulmonary arterial pressure; RV, right ventricle; SAP, systemic arterial pressure

Introduction

The change in lung expression of nitric oxide synthase (NOS) in response to chronic hypoxia (CH) has extensively been studied in the rat. Northern and Western blot analyses in hypoxic rats have demonstrated increased lung tissue expression of mRNA and protein for endothelial NOS (eNOS) (Xue *et al.*, 1994; Shaul *et al.*, 1995; Le Cras *et al.*, 1996; 1998; Xue & Johns, 1996; Tyler *et al.*, 1999), inducible NOS (iNOS) (Xue *et al.*, 1994; Le Cras *et al.*, 1996; Xue & Johns, 1996), and neuronal NOS (nNOS) (Xue & Johns, 1996). The significant increases in gene and protein expression were observed as early as 24 h after hypoxia (Xue & Johns, 1996). NOS immunohistochemistry has shown that the hypoxic increase in eNOS staining intensity is induced in the pulmonary arteries (diameter 50–300 μm) but not in veins (60–300 μm) (Resta *et al.*, 1997). On the other hand, iNOS increased in vascular smooth muscle at all levels of hypoxic pulmonary vessels, although it was very limited in normoxic pulmonary vessels (Xue *et al.*, 1994; Xue & Johns, 1996). Moreover, the majority of nNOS immunoreactivity was distributed in bronchial epithelial cells, although it was found in the neurons surrounding the large bronchi (Xue & Johns, 1996).

The functional role of endogenous nitric oxide (NO) in modulating pulmonary vascular tone of the CH rat has been examined chiefly by use of isolated perfused lungs or isolated proximal elastic pulmonary arteries (main or extralobar pulmonary arteries). Most, but not all (Adnot *et al.*, 1991; Eddahibi *et al.*, 1992), pressure-flow studies of hypoxic lungs have suggested either normal or increased responsiveness to the nonselective NOS inhibitor (Barer *et al.*, 1993; Russ &

*Author for correspondence; E-mail: mshirai@ri.ncvc.go.jp

Walker, 1993; Isaacson *et al.*, 1994; Roos *et al.*, 1996; Muramatsu *et al.*, 1997; Tyler *et al.*, 1999) and to endothelium-dependent vasodilators (Barer *et al.*, 1993; Russ & Walker, 1993; Isaacson *et al.*, 1994; Muramatsu *et al.*, 1996; Resta & Walker, 1996; Roos *et al.*, 1996). In contrast, isolated proximal arteries have impaired responsiveness to endothelium-dependent vasodilators (Crawley *et al.*, 1992; Rodman, 1992; Carville *et al.*, 1993; Shaul *et al.*, 1993; Maruyama & Maruyama, 1994). These data suggest the possibility that the effect of CH on endogenous NO-mediated vasodilatation differs between the muscular (resistance) and elastic (conduit) pulmonary vessels in the rat. Recently, using a selective iNOS inhibitor, a pressure-flow study has suggested that NO derived from iNOS does not modulate pulmonary vasoconstrictor responsiveness in isolated lungs from CH rats (Resta *et al.*, 1999).

Despite such extensive structural and functional studies, the following problems have yet to be examined sufficiently in the CH rat. One issue is whether, and to what extent, the effect of hypoxia on the NO-mediated basal vascular tone regulation varies along the series-connected small pulmonary arteries, from elastic to muscular segment levels and, moreover, between the parallel-arranged vascular branches within each vascular segment level. Another is whether the increased iNOS and nNOS can contribute to the basal tone regulation in these small arteries. To resolve these issues, we applied a specially designed X-ray television system (Sada *et al.*, 1985; Shirai *et al.*, 1986) on anaesthetized rats and directly measured internal diameter (ID) changes due to NOS inhibition in the pulmonary arterial trees (100–700 μm ID), which contain both muscular and distal elastic segments (Kay, 1983; Sasaki *et al.*, 1995). We used the *in vivo* pulmonary circulation associated with natural blood perfusate and flow pattern, because these are important factors for determining the expression of NO activity (Hakim, 1994; Sprague *et al.*, 1995). The ID changes were compared between 4-week hypoxic rats and normoxic control rats. N^{ω}-nitro-L-arginine methyl ester (L-NAME) or N^{ω}-monomethyl-L-arginine (L-NMMA) was used for nonselective NOS inhibition, L-canavarine or *S*-methylisothiourea sulphate for selective inhibition of iNOS (Szabo *et al.*, 1994; Teale & Atkinson, 1994; Liaudet *et al.*, 1996) and 7-nitro indazole for selective inhibition of nNOS (Moore *et al.*, 1993; Kalisch *et al.*, 1996; Okamoto *et al.*, 1997). We found that nonselective NOS inhibition and iNOS-selective inhibition cause significant ID changes, but nNOS-selective inhibition does not. Therefore, after these physiological studies, we further analysed eNOS and iNOS immunohistochemical localization in the pulmonary arteries to examine the correspondence between the structural and functional upregulation of NOS.

Methods

The study was conducted in accordance with the Guiding Principles for the Care and Use of Animals in the Field of Physiological Sciences, published by the Physiological Society of Japan. Male Sprague–Dawley rats were used for all experiments.

Chronic environment

Rats aged 6 weeks at the start of the experiment were placed in either a normobaric environmental chamber maintained at 10% O_2 (hypoxic group, $n=15$) or a chamber open to room air (control normoxic group, $n=11$) for 4 weeks. Carbon dioxide was removed by self-indicating soda lime granules and excess humidity prevented by cooling of the recirculation circuit. The environment within the chamber was monitored with a mass spectrometer. All hypoxic and normoxic rats were kept in the same room, at the same light–dark cycle. Food and water were available *ad libitum*. The chamber was opened for ~10 min daily to clean the cages and replenish food and water.

Experimental procedure and angiography

Rats were anaesthetized with pentobarbital sodium (50 mg kg^{-1} i.p.) and supplemental doses (10–20 mg kg^{-1} h^{-1} i.v.) were administered to maintain an appropriate level of anaesthesia. Each rat was intubated with an endotracheal tube and artificially ventilated with room air. A *syrustic* catheter (outer diameter, ~500 μm) was introduced from the right jugular vein into the left main pulmonary artery. Another catheter was inserted into the right femoral artery. Thereafter, the left-side rib cage was partially excised to expose directly the left lung to the X-ray. The end-expiratory pressure was adjusted to 3.0 cm H_2O to prevent lung collapse. Heparin sodium (500 IU kg^{-1}) was administered to prevent blood coagulation.

The system and experimental set-up used in the angiography have been described previously in detail (Sada *et al.*, 1985; Shirai *et al.*, 1986). Briefly, the rat was placed inside an X-ray apparatus box (Hitex) and fixed in such a manner that the exposed left lobe automatically came into contact with a plate just above the beryllium faceplate of an X-ray-sensitive, 1-in. vidicon camera (Hamamatsu Photonics). During temporary cessation of ventilation for ~3 s at end expiration, a contrast medium (0.2 ml, 60% Urografin) was injected into the main pulmonary artery at a constant speed (0.15 ml s^{-1}), and its passage through the pulmonary vascular bed recorded serially at high speed (30 frames s^{-1}) on a videotape recorder (PVW-2800, Sony). During the experiment, the temperature in the box was maintained at 25–28°C, and the surface of the exposed lung kept wet by warm (37°C) saline. Blood gases and pH were examined by a blood gas analyzer (ABL-2, Radiometer).

ID measurement

The serial angiograms recorded on the videotape recorder were then transferred to a digital image processor (DVS-5000, Hamamatsu). To obtain the arteriogram for measuring ID, two to three serial frames within a diastolic phase, in which vascular trees were extensively filled with contrast medium, were added up and averaged by the digital image processor. The processed image was electrically transferred to an image hard copy unit (model 4634, Sony Tektronix) and copied clearly onto paper. The ID of the pulmonary vessels on the copy was then measured manually using a digitizer (model 9874A, Hewlett-Packard) connected to a minicomputer. The readers of the angiograms were blinded to the treatment protocol.

Analysis of ID response

Following the method we described in a previous study (Shirai *et al.*, 1986), we took a random selection of many vascular sites

for the ID measurements. The ID percentage change in response to an NOS inhibitor was calculated at each measured vascular site. These sites were classified into three vascular groups, that is the muscular arteries (100–300 μm ID), smaller transitional elastic arteries (400–500 μm), and larger classical elastic arteries (600–700 μm), according to their vascular branching pattern and baseline ID sizes (Kay, 1983; Sasaki *et al.*, 1995). By pooling all the data within a vascular group, the mean value of the ID percentage change was obtained in each of the three groups. The ID responses were separated into three types (constriction, dilatation, and no change) according to the following definition: an increase or decrease more than 5% in the percentage ID change is defined as dilatation or constriction, respectively, and a change below 5% as no change.

In the present study, the mean pulmonary arterial pressure (PAP) of the CH rat was ~3 mmHg larger than that of the control rat under baseline conditions, suggesting that the baseline ID at the same serial segments of arteries may differ between these rats. Therefore, we compared the baseline ID of primary branches (400–600 μm) arising from the axial artery or peripheral branches (<300 μm) arising from the primary branch (Sasaki *et al.*, 1995) between these rats. However, there was no significant difference in the mean baseline ID value at any of the serial segments.

Experimental protocols for angiography

In each of the hypoxic and normoxic groups, the baseline angiogram was recorded first, and then an injection of nonselective NOS inhibitor ($n=4$), L-NAME (50 mg kg^{-1} i.v., $n=2$) or L-NMMA (60 mg kg^{-1} i.v., $n=2$), an injection of iNOS selective inhibitor ($n=4$), L-canavanine (100 mg kg^{-1} i.v., $n=2$) or *S*-methylisothiourea sulphate (3 mg kg^{-1} i.v., $n=2$), or an injection of nNOS selective inhibitor, 7-nitro indazole (50 mg kg^{-1} i.p., $n=3$), was performed. The angiograms following the injection of a nonselective NOS inhibitor or an iNOS selective inhibitor were taken ~20 min after the injection ended. Similarly, the angiogram was recorded 30–40 min after the injection of an nNOS selective inhibitor. In our preliminary dose–response data, the doses of NOS inhibitors were enough to cause maximal levels of ID reduction. Moreover, the magnitudes and distribution patterns of the ID reduction caused by the two chemically different nonselective NOS inhibitors, as well as the two iNOS inhibitors, were similar. Therefore, we considered that nonspecific effects other than those due to NOS inhibition are negligibly small in the doses used in the present study and that pooling the data from the two different inhibitors is reasonable.

We found significant ID reductions after the injections of a nonselective NOS inhibitor and an iNOS selective inhibitor, but not after nNOS selective inhibitor injection. To examine whether these ID constrictions primarily resulted from inhibiting the release of NO derived from L-arginine, the third angiogram following the addition of L-arginine (100–200 mg kg^{-1} i.v.) was further recorded in the rats given a nonselective NOS inhibitor or an iNOS selective inhibitor.

In the current study, PAP increased by ~3 mmHg after the nonselective NOS inhibitor administration in the CH rat. It is thus possible that the pressure-sensing mechanism (see Discussion) influenced the ID change pattern in response to the inhibitor. To examine this possibility, we measured the effects of mechanically induced PAP increase on the ID of pulmonary arteries in CH rats ($n=4$). PAP was increased ~4 mmHg above the baseline value by partially interrupting blood flow into the right side of the lungs. The angiogram of the left lung was recorded at the time when the PAP increase was maintained for 50–60 s periods.

There was an interval of ~15 min between each angiography to eliminate any influence of the contrast medium. All experiments were finished within a few hours of removal from the chamber.

Immunohistochemistry and histology

Within the rats that had been used for recording angiograms with nonselective NOS inhibition and iNOS selective inhibition, immunolocalization of NOS proteins in the pulmonary arteries was performed. Four out of eight hypoxic rats and four out of eight normoxic rats were employed. After putting marks on the left lung regions, where the ID changes had been measured, the lungs were isolated from the rats under anaesthesia. Cannulas were inserted into the pulmonary artery and left atrium, and the lungs were perfused with heparinized phosphate-buffered saline (PBS) followed by 4% paraformaldehyde in 0.1 M PBS (pH 7.3). Simultaneously, the lungs were inflated via the trachea to a pressure of 23 cm H_2O with 4% paraformaldehyde and then placed in 10% buffered formaline for paraffin embedding. The left lung tissues that had been marked were cut into 7–9-mm sections. Paraffin sections 2 μm thick were mounted onto precleaned slides (Superfrost Plus; Fisher Scientific, Springfield, NJ, U.S.A.), dewaxed in 100% xylene, and then rehydrated in graded alcohol solutions. Throughout the protocol, slides were washed, as appropriate, in PBS. Antigen retrieval was performed by microwave treatment and proteinase K treatment for eNOS and iNOS immunostaining, respectively. Sections were treated with 0.3% H_2O_2 (30 min) to inhibit endogenous peroxidases and incubated with normal serum (30 min) to reduce nonspecific binding of secondary antibodies. Sections were then incubated at 4°C overnight with either of two anti-NOS antibodies: (1) a mouse monoclonal antibody raised against a peptide fragment of amino acids 1030–1209 of human eNOS (1:3000 dilution; Transduction Laboratories, Lexington, KY, U.S.A.) or (2) a rabbit polyclonal antibody raised against a synthetic peptide corresponding to amino-acid residues 1131–1144 (with one additional N-terminal cysteine) of mouse macrophage iNOS (1:3000 dilusion; Alexis Corporation, Lausen, Switzerland). The anti-eNOS antibody was characterized for use in Western blot analysis (identifying protein bands at 140 kDa for eNOS), and showed wide species reactivity, including reactivity with human and rat NOS (Transduction Laboratories). The anti-iNOS antibody was also characterized by Western blot (identifying a band at 130 kDa) and showed reactivity with human and rat NOS (Alexis Corporation). After washing off unbounded primary antibodies, sections were incubated with secondary biotinylated antibodies against mouse or rabbit (DAKO Co., Japan) (30 min), followed by incubation in avidin/biotin/horseradish peroxidase complex (DAKO Co., Japan) (30 min). Subsequently, peroxidase activity was visualized by incubation (3 min) with 0.05% 3,3′-diaminobenzidine (DAKO Co., Japan), which gives a brown reaction product. The reaction was stopped by washing with

water. The slides were then counterstained with Mayer's haematoxylin, dehydrated, and mounted. For negative control studies, slides were incubated with mouse IgG (for monoclonal antibodies) or rabbit IgG (for polyclonal antibodies) instead of primary antibody. No staining was observed in these negative control sections. Serial sections were stained with elastic Van Gieson's method to distinguish arteries and veins by the presence of an internal elastic lamina (Resta *et al.*, 1997).

According to the classification proposed by Sakai *et al.*, the elastic and muscular arteries were distinguished by the structure of the media. Vessel diameters were calculated from their external circumference. Oblique sections in which the elastic laminae were indistinct at one or more points on the circumference were excluded from analysis. Slides were examined independently by three blinded reviewers and vessels counted for NOS-positive or NOS-negative staining.

Statistical methods

The significance of differences in ID values and haemodynamic data between the conditions of baseline and NOS inhibition (among the values of baseline, NOS inhibitor alone, and NOS inhibitor + L-arginine) was tested by a paired *t*-test (analysis of variance (ANOVA) and Scheffe's test). The differences in the ID and haemodynamic data between control and hypoxic groups were examined by an unpaired *t*-test. ID response differences among the different serial vascular segments were assessed by analysis of variance (ANOVA) and Scheffe's test. All data are expressed as mean ± s.e.m., and $P<0.05$ was considered significant.

Results

Baseline values of body and right ventricle (RV) and left ventricle weight, and blood gases in control and CH rats

The mean values of body weight, (right ventricle (RV)/left ventricle (LV) + septum) ratio, and systemic arterial blood $P_{O_2}(Pa_{O_2})$, $P_{CO_2}(Pa_{CO_2})$ and pH are compared between the control and CH rats (Table 1). Blood gases were measured during normoxic ventilation. Final body weight was ~30 g smaller in the CH rat than in the control rat, while RV/(LV + septum) ratio ~0.30 larger. There were no significant differences in blood gases between these rats.

Haemodynamic responses due to NOS inhibition

Mean PAP and mean systemic arterial pressure (SAP), before and after NOS inhibitor injection, are compared between the control and CH rats (Table 2). These parameters were measured just before injection of the contrast medium under normoxic ventilation. In the CH rat, the nonselective NOS inhibitors significantly increased PAP and SAP by 3.2 and 34 mmHg, respectively. In the normoxic rat, these inhibitors caused a significant increase (30 mmHg) only in SAP. In contrast, the iNOS and nNOS selective inhibitors significantly changed neither PAP nor SAP in both control and CH rats.

Table 1 Baseline values of body weight, RV/(LV + septum) weight ratio, and blood gases during normoxic ventilation

Parameters	*Control rats (n = 11)*	*4-wk hypoxia rats (n = 11)*
Initial body weight (g)	197 ± 2	196 ± 2
Final body weight (g)	327 ± 7	299 ± 5*
RV/(LV + septum) ratio	0.33 ± 0.03	0.62 ± 0.05**
pH	7.41 ± 0.02	7.37 ± 0.04
PO_2 (Torr)	96 ± 6	93 ± 5
PCO_2 (Torr)	33 ± 2	35 ± 2

Values are mean ± s.e.m. *$P<0.05$; **$P<0.01$ vs control rats.

Table 2 Mean pulmonary arterial pressure (PAP) and systemic arterial pressure (SAP) before and after NOS inhibitor injection

Blood pressure (mmHg)	*Control rats*	*4-week hypoxia rats*
(1) *Nonselective NOS inhibition (NNI)*		
PAP (baseline)	18.0 ± 0.5	21.1 ± 1.0*
PAP with NNI	18.6 ± 0.6	24.3 ± 1.1*, **
PAP with NNI + L-arginine	17.9 ± 0.6	23.3 ± 1.2*
SAP (baseline)	93 ± 6	101 ± 7
SAP with NNI	123 ± 7**	135 ± 9**
SAP with NNI + L-arginine	98 ± 7	108 ± 9
(2) *iNOS selective inhibition (ISI)*		
PAP (baseline)	17.2 ± 0.6	22.1 ± 1.1*
PAP with ISI	17.4 ± 0.7	22.9 ± 1.1*
PAP with ISI + L-arginine	17.1 ± 0.7	22.2 ± 1.1*
SAP (baseline)	96 ± 6	105 ± 7
SAP with ISI	98 ± 6	113 ± 8
SAP with ISI + L-arginine	94 ± 7	107 ± 8
(3) *nNOS selective inhibition (NSI)*		
PAP (baseline)	18.0 ± 0.5	22.4 ± 1.0*
PAP with NSI	18.2 ± 0.5	22.6 ± 1.0*
SAP (baseline)	94 ± 6	102 ± 7
SAP with NSI	96 ± 6	105 ± 7

Values are mean + s.e.m. The mean value in classes 1 and 2 was obtained by pooling all the data in response to two different nonselective NOS inhibitors and two iNOS-selective inhibitors, respectively. *$P<0.05$ vs control rats. **$P<0.05$ vs baseline.

Regional changes in NOS-inhibitor induced responses in parallel- and series-arranged pulmonary arteries following 4-week hypoxia

Figure 1 shows typical ID changes of small pulmonary arteries in response to L-NMMA injection in the control and CH rats. On injection, slight ID decreases were induced in the control rat. In the CH rat, in contrast, clear ID decreases occurred in many branches, particularly smaller branches.

The mean value of the NOS inhibitor-induced ID change at each level of the muscular, transitional elastic, and classical elastic arteries is shown in the control and CH rats (Figure 2). During nonselective NOS inhibition (left), the ID of all these arteries significantly constricted in both control and CH rats. The ID constriction of the muscular arteries was significantly ($P<0.05$) smaller than those of the transitional and classical elastic arteries in the control rat. Comparing the ID constric-

tion due to nonselective NOS inhibition between the control and CH rats, there was a large difference in the muscular arteries and a small but significant difference in the transitional elastic arteries, whereas no significant difference was present in the classical elastic arteries. On the other hand, during iNOS selective inhibition (right), no significant ID response was induced in any of the arteries in the control rat. However, in the CH rat, a significant ID constriction occurred locally in the muscular arteries. Therefore, a significant difference between the control and CH rats was restricted in these arteries. During nNOS selective inhibition, no significant ID response was observed at any of the muscular and elastic arteries in the control and CH rats. The mean values of ID changes for the muscular, transitional elastic, and classical elastic arteries of the control rat were 0 ± 2, 2 ± 2, and $1\pm2\%$, respectively, and those of the CH rat were 3 ± 2, 1 ± 2, and $3\pm2\%$, respectively.

After making an L-arginine injection, the ID decreases due to nonselective NOS inhibition and iNOS selective inhibition were completely abolished in both control and CH rats. The mean values of ID percentage changes in response to nonselective NOS inhibitor + L-arginine in the muscular, transitional elastic, and classical elastic arteries were -2 ± 4, 2 ± 4, and $4\pm3\%$, respectively, in the control rat, and were -3 ± 4, -1 ± 4, and $2\pm4\%$ for the CH rat, respectively. The mean values of ID percentage changes in response to iNOS selective inhibitor + L-arginine in the three levels of vessels were 3 ± 4, 4 ± 4, and $1\pm4\%$, respectively, in the control rat, and were 1 ± 4, 3 ± 4, and $-2\pm4\%$ for the CH rat, respectively.

Relative frequency distribution of ID response due to NOS inhibition is compared between the control and CH rats (Figure 3). During nonselective NOS inhibition (left panels),

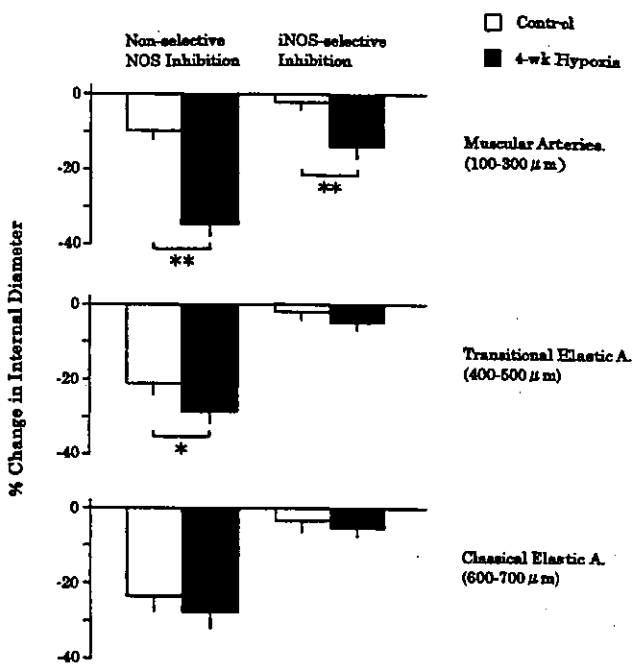

Figure 2 Mean values of NOS inhibitor-induced ID changes for muscular, transitional elastic, and classical elastic pulmonary arteries are shown in control (open column) and chronically hypoxic (solid column) rats. CH greatly enhanced ID reductions due to nonselective NOS inhibition (left) and iNOS-selective inhibition (right) primarily in muscular pulmonary arteries. $^{*}P<0.05$, $^{**}P<0.01$ vs control.

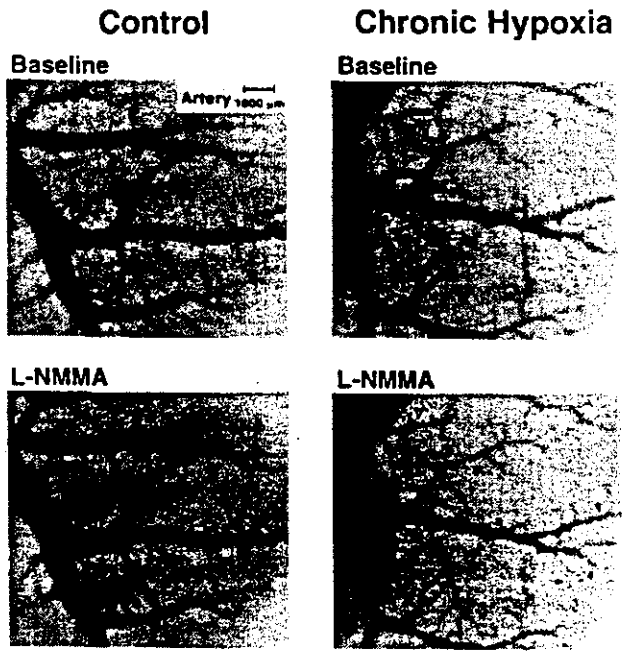

Figure 1 Typical angiograms of small pulmonary arteries obtained before (top panels) and after (bottom panels) nonselective NOS inhibitor (L-NMMA) injection in control (left panels) and chronically hypoxic (right panels) rats. Clear vasoconstrictions are chiefly observed in more distal side vessels $\lesssim 300\,\mu m$ (arrowheads).

the frequency curves of the control and CH rats were very different in the muscular arteries (100–300 μm), but not in the transitional (400–500 μm) and classical (600–700 μm) elastic arteries. In the muscular arteries, the peaks of the control and CH curves were observed at 5–15 and 35–45% constriction, respectively. Moreover, ~40% of ID responses were no change in the control vessels, but almost all ID responses were significant constriction in the CH vessels. In the transitional and classical elastic arteries, almost all ID responses were significant constriction in both control and CH vessels. The peaks of the control and CH distributions in the transitional arteries were at 15–25 and 25–35% constriction, respectively, but those for classical arteries were about the same level (25–35% constriction).

During iNOS selective inhibition (right panels), a clear difference between the control and CH response distributions existed only in the muscular arteries. In these arteries, the peaks of the control and CH curves were observed at no change and 5–15% constriction, respectively. Significant constriction was only ~20% of the ID responses in the control distribution, but ~60% in the CH. However, it is noteworthy that, in contrast to the case of nonselective NOS inhibition, ~40% of muscular artery responses were still no change in the CH rat. In the elastic arteries, just as in the muscular arteries, ~80% of the ID responses in the control distribution curve were no change, and the curves of the control and CH rats displayed similar patterns.

During nNOS selective inhibition, more than 95% of the ID responses were no change and the remaining responses, if any, were small constrictions in both the control and CH rats.

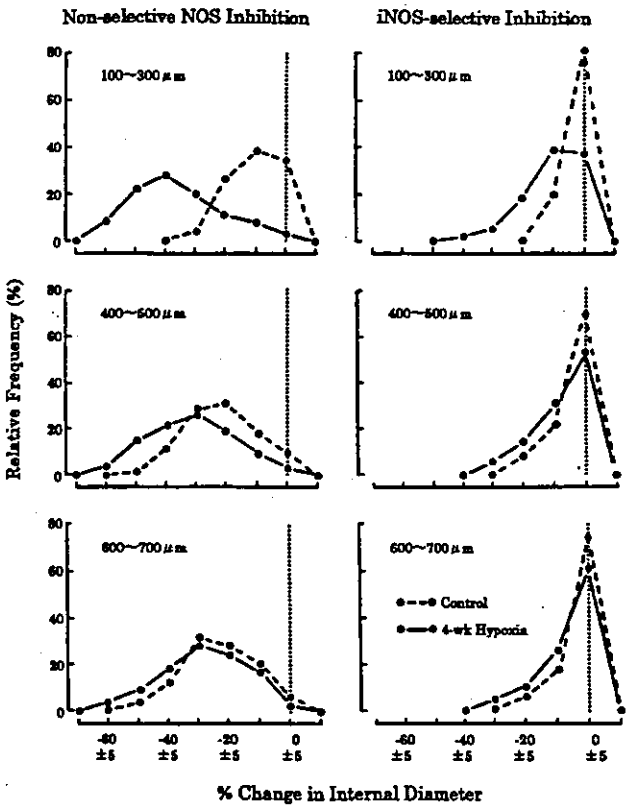

Figure 3 Relative frequency distributions of ID changes due to nonselective NOS inhibition (left) and iNOS-selective inhibition (right) are shown in control (broken line) and chronically hypoxic (solid line) rats. Dotted line indicates no ID change as defined in Methods section. Clear difference in distribution pattern between control and hypoxic rats is seen primarily in muscular pulmonary arteries (100–300 μm) in both types of NOS inhibition.

Effects of PAP increases due to nonselective NOS inhibition on ID

The mechanically induced ~4 mmHg PAP increase had no significant effect on the ID of the muscular and elastic arteries in the CH rat. The mean value of percentage ID change due to the PAP increase for all these arteries was 3±3%.

NOS immunoreactivity changes

Figure 4 shows representative photographs of eNOS immunostaining in the small muscular pulmonary arteries from the control (a) and CH (b) rats. eNOS immunoreactivity was detected in the endothelium of hypoxic arteries (Figure 4b) but not in the control arteries (Figure 4a). Figure 5 shows typical examples of iNOS immunostaining of CH and control rat lungs. The low-magnification view of the hypoxic lung (Figure 5a) showed that an iNOS immunopositive muscular pulmonary artery (arrow) and an iNOS-immunonegative muscular artery (arrowhead) are simultaneously observed in the same section. In the higher-magnification view, the former artery displayed strong iNOS immunostaining primarily in the smooth muscle layers (Figure 5b). However, the latter showed no immunostaining even with higher magnification (Figure 5c). iNOS immunoreactivity was not detected in the control arteries (arrowhead in Figure 5d).

The quantitative data on the distribution of NOS immunoreactivity in the pulmonary arteries of control vs CH lungs are shown in Table 3. In control lungs, eNOS immunoreactivity was distributed only in 9–51% of the muscular arteries, although 91% of the elastic arteries were positive for eNOS. However, the percentage of eNOS-positive vessels greatly increased up to 89–94% in the muscular arteries of CH lungs, while the increase was slight (7%) in the elastic arteries. On the other hand, the percentage of iNOS-positive vessels was small (<10%) in both muscular and elastic arteries of control lungs and increased only to 44–55 and to 68% in these arteries of CH lungs.

Discussion

We quantitatively measured the ID changes of the muscular (resistance) and elastic (conduit) pulmonary arteries in response to different types of NOS inhibitors using an X-ray television system on the control and CH rats under anaesthesia. Moreover, we conducted immunohistochemical analyses to localize NOS proteins in the pulmonary arteries within the control and CH lungs where the ID changes were examined. This was performed to investigate the possible contributions of the hypoxia-induced increase in NOS expres-

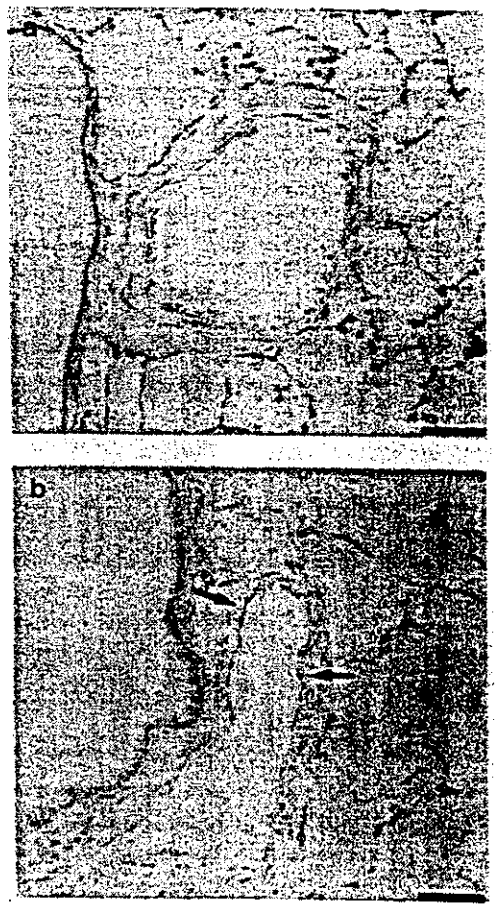

Figure 4 eNOS immunostaining of small muscular pulmonary arteries of control (a) and chronically hypoxic (b) rats. eNOS protein was detected in endothelium of hypoxic arteries (arrows), but not in control arteries. Scale bars = 50 μm.

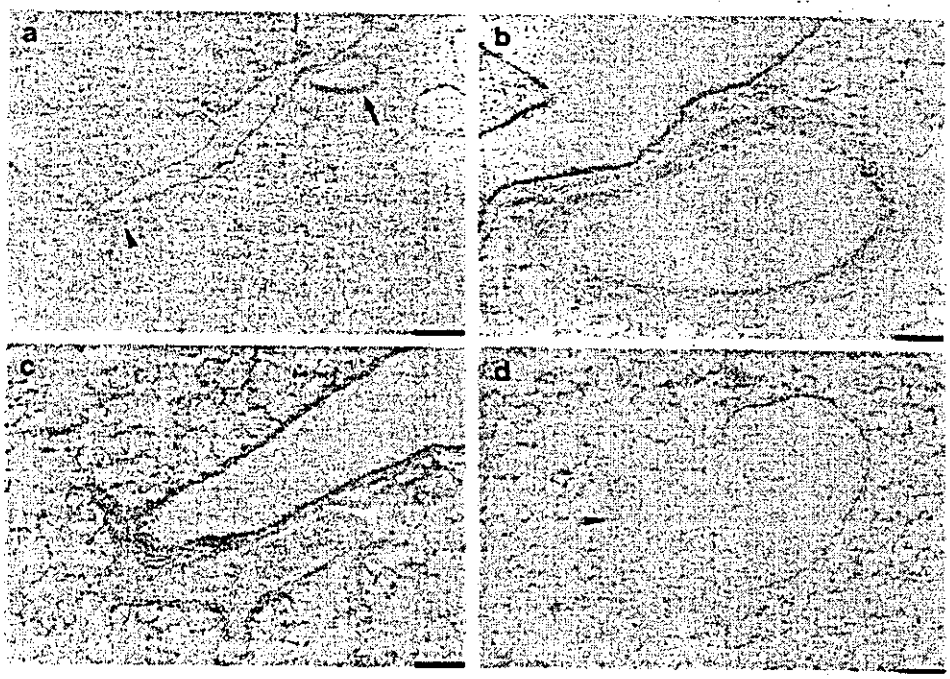

Figure 5 iNOS immunostaining of muscular pulmonary arteries of chronically hypoxic (a–c) and control (d) rats. (a) Low magnification view. iNOS-positive (arrow) and iNOS-negative (arrowhead) muscular pulmonary arteries are seen in the same section. (b, c) Higher magnification views of iNOS-positive and iNOS-negative arteries, respectively. (d) iNOS-negative muscular artery (arrowhead). Scale bars: (a) 500 μm, (b, c) 50 μm, (d) 100 μm.

Table 3 Pulmonary arteries positive and negative for NOS

	Elastic (400–700 μm)		*Muscular* (100–300 μm)		*Muscular* (<100 μm)	
	Positive	*Negative*	*Positive*	*Negative*	*Positive*	*Negative*
eNOS						
C	39 (90.7)	4 (9.3)	56 (50.9)	54 (49.1)	23 (8.9)	236 (91.1)
CH	43 (97.7)	1 (2.3)	97 (94.2)	6 (5.8)	210 (88.6)	27 (11.4)
iNOS						
C	4 (9.8)	37 (90.2)	7 (6.0)	109 (94.0)	4 (1.6)	252 (98.4)
CH	30 (68.2)	14 (31.8)	56 (55.4)	45 (44.6)	104 (43.7)	134 (56.3)

Values are presented as number (%). Number of NOS-positive and NOS-negative vessels was counted in control (C; $n=4$) and 4-week hypoxic (CH; $n=4$) rats.

sion to regulating tone at individual pulmonary arterial branches with natural blood circulation.

RV hypertrophy

The presence of pulmonary hypertension in rats breathing hypoxic air was reflected in an increased ratio of RV/LV + S, which averaged 0.62 ± 0.05 vs 0.33 ± 0.02 in normoxic controls. These ratios in the CH and control rats agree with those of others (Abraham *et al.*, 1971; Rabinovitch *et al.*, 1979; Muramatsu *et al.*, 1997).

ID constriction mechanisms in pulmonary arteries in response to NOS inhibitor injection

We showed that L-arginine injection completely abolishes the ID reductions in response to nonselective NOS inhibitors and iNOS selective NOS inhibitors in the pulmonary arteries. This suggests that inhibiting the basal release of NO derived from L-arginine is primarily responsible for the ID constrictions.

In the present study, L-NAME (50 mg kg^{-1} mg kg^{-1} i.v.) or L-NMMA (60 mg kg^{-1} i.v.) was used for nonselective NOS inhibition and L-canavanine (100 mg kg^{-1} i.v.) or *S*-methylisothiourea sulphate (3 mg kg^{-1} i.v.) for selective iNOS inhibition. We determined the doses of NOS inhibitors based on the previous data (Loeb & Longnecker, 1992; McCormack & Paterson, 1993; Oka *et al.*, 1993; Huang *et al.*, 1994; Szabo *et al.*, 1994; Teale & Atkinson, 1994; Liaudet *et al.*, 1996) and our preliminary dose–response data (see Methods). Previous studies (Teale & Atkinson, 1994; Liaudet *et al.*, 1996) have shown that L-canavanine (100 mg kg^{-1} i.v.) almost completely suppresses the lipopolysaccharide-induced hypotension in anaesthetized rats, although it does not significantly affect blood pressure in the absence of lipopolysaccharide. *S*-methylisothiourea sulphate (3 mg kg^{-1} i.v.) caused a potent pressor response in lipopolysaccharide-treated rats as com-

pared with control rats and a restoration of blood pressure to prelipopolysaccharide levels (Szabo *et al.*, 1994). The present study has shown a significant ID reduction in the CH rat, but no significant response in the control rat in response to L-canavanine and *S*-methylisothiourea sulphate. From these previous and present data, it seems reasonable to assume that the doses of iNOS inhibitors we employed were adequate to inhibit iNOS, but with minor effects on the other types of NOS *in vivo*.

For nNOS selective inhibition, we used 7-nitro indazole ($50\,mg\,kg^{-1}$ i.p.). These doses of the inhibitor were able to cause 60–80% reduction of nNOS activity in the rat (Kalisch *et al.*, 1996; Okamoto *et al.*, 1997), suggesting that the doses of nNOS inhibitor were also adequate to inhibit nNOS in the current study. Therefore, our finding that 7-nitro indazole had no significant effect on any pulmonary arteries (100–700 μm) of the control and CH rats is likely to mean that the role of nNOS in controlling the vascular tone of these vessels is minimal, if any at all. This is consistent with the immunohistochemical data that nNOS immunoreactivity was not detected in the small pulmonary vessels of normoxic and CH rats (Xue & Johns, 1996) and with the physiological data of no significant contribution of nNOS to modulating pulmonary vascular tone in the mouse (Fagan *et al.*, 1999b) and cat (Shirai *et al.*, 1999). Our result also suggests that sympathetic nerve activity increase caused by nNOS inhibition in the brain stem (Umans, 1995) contributed little to the nonselective NOS inhibitor-induced ID reduction.

The contribution of pressure- and flow-sensing mechanisms (Bevan & Laher, 1991) to the NOS inhibitor-induced ID response has been discussed. There was a PAP elevation of ~3 mmHg in response to nonselective NOS inhibitors in the CH rat (Table 2), suggesting the possibility that the pressure-sensing mechanism influenced the ID change pattern caused by the local action of nonselective NOS inhibitor on the small pulmonary arteries. To examine this possibility, we measured ID changes of the pulmonary vessels in response to mechanically induced increases in PAP. No significant ID change was found in response to ~4 mmHg PAP rise, suggesting that this possibility is small.

Pulmonary blood flow was not measured in this study, but it was reported that cardiac output decreases by 15–40% in response to nonselective NOS inhibitor in normoxic (Loeb & Longnecker, 1992; McCormack & Paterson, 1993; Oka *et al.*, 1993; Huang *et al.*, 1994) and chronically hypoxic rats (Oka *et al.*, 1993) and did not significantly change with iNOS selective inhibitors in these rats (Liaudet *et al.*, 1996; Resta *et al.*, 1999). Therefore, another possibility is that the flow-sensing mechanism affected the ID change pattern in response to nonselective NOS inhibitor administration. However, in preliminary experiments, we found no significant ID change in response to ~40% decrease in pulmonary blood flow caused by partially occluding the circumference of inferior vena cava with a 4-0 silk ligature. This suggested that this possibility is also small.

However, these results cannot completely exclude these possibilities, since we did not determine the local pressure- and flow-mediated vasomotor responses at different serial segments of the pulmonary vessels. To determine these responses, it would be necessary to measure directly the local pressure and flow velocity at the same site where vascular dimensions are being assessed.

Contribution of endogenous NO to controlling basal pulmonary vascular tone in normoxic rats

Previous pressure-flow studies have shown that nonselective NOS inhibitors increase basal pulmonary vascular resistance in intact and isolated lungs of the lamb, pig, rabbit, cat, and man (Persson *et al.*, 1990; Fineman *et al.*, 1991; McMahon *et al.*, 1991; Gordon & Tod, 1993; Nelin & Dawson, 1993; Cremona *et al.*, 1994; Stamler *et al.*, 1994; Albertini *et al.*, 1996), although no effect in the dog (Nishiwaki *et al.*, 1992; Cremona *et al.*, 1994; Leeman *et al.*, 1994). This suggests that endogenous NO plays a contributory role in regulating basal pulmonary vascular tone for all these animals except the dog (Barnes & Liu, 1995). On the other hand, in the rat, this problem has mainly been studied using isolated perfused lungs, but with inconsistent results. Many investigators have shown no or little effect of nonselective NOS inhibitors on the basal pulmonary vascular resistance (Robertson *et al.*, 1990; Hasunuma *et al.*, 1991; Barer *et al.*, 1993; Hampl *et al.*, 1993; McCormack & Paterson, 1993; Russ & Walker, 1993; Isaacson *et al.*, 1994; Resta *et al.*, 1999), although others have shown a significant effect (Barnard *et al.*, 1993; Roos *et al.*, 1996; Cadogan *et al.*, 1999). In the present study, we considered the change in ID to be better explained as an index of local vasomotor response in a given vessel than the change in calculated resistance estimated from the pressure–flow relation. Therefore, we directly measured ID changes of the rat pulmonary arteries using an X-ray TV system (Sada *et al.*, 1985; Shirai *et al.*, 1986). Our data showed that nonselective NOS inhibitor injection causes a significant ID reduction in both muscular (100–300 μm) and elastic (400–700 μm) segment levels in normoxic control rats (Figure 2). Relative frequency distribution of ID response showed that the peak of the frequency curve of the elastic arteries is located on the more constrictor side than that of the muscular arteries, and that the constrictor response occurs in most of the elastic arteries but only in about half of the muscular arteries (Figure 3). This suggests greater effects of NO on basal tone of the elastic pulmonary arteries and lesser effects for the muscular arteries in the normoxic rat. Moreover, there was the coexistence of relatively small magnitudes of constrictions and no change with similar frequencies among parallel-arranged muscular arteries (Figure 3). This ID response pattern may partly explain the previous data of no or little change in the pressure–flow relation of the entire lung (Robertson *et al.*, 1990; Hasunuma *et al.*, 1991; Barer *et al.*, 1993; Hampl *et al.*, 1993; McCormack & Paterson, 1993; Russ & Walker, 1993; Isaacson *et al.*, 1994; Resta *et al.*, 1999) and the present data of no significant PAP rise in response to nonselective NOS inhibition, if we assume that local redistributions of blood flow from constricted to nonconstricted muscular arteries occurred and then recruited new peripheral channels such as capillaries, maintaining entire pulmonary vascular resistance within nearly baseline levels. In addition, because the previous pressure–flow studies were mostly performed in constant perfused lungs, a decrease in NO production due to the artificial perfusate composition (Sprague *et al.*, 1995) and/or mechanical flow pattern (Hakim, 1994) may have occurred in these studies, making it more difficult to detect the small magnitude of vasoconstriction due to NOS inhibition in the muscular arteries.

The present study also demonstrated that selective inhibitors of iNOS had no significant effects on any levels of the arteries observed in control rats (Figure 2). Relative frequency distribution of ID response showed that iNOS selective inhibition causes no ID changes in ~80% of the muscular and elastic arteries, and small magnitudes of ID constriction in the remaining arteries (Figure 3). The data suggest a minor contribution of iNOS-derived NO to basal tone regulation in both muscular and elastic arteries, and probably explain the findings that selective iNOS inhibition had no effect on the baseline pulmonary vascular resistance in the rat (Resta *et al.*, 1999). Moreover, considering in connection with the above-mentioned suggestion of minor role of nNOS in regulating vascular tone of the muscular and elastic arteries, the present study suggests that, during normoxia, the predominant isoform of NOS regulating basal tone of these arteries is eNOS. This is consistent with the findings in the mouse that baseline pulmonary arterial pressure in eNOS null lungs significantly increased compared with wild type (Steudel *et al.*, 1997; Fagan *et al.*, 1999b), but the pressure in iNOS null lungs and nNOS null lungs did not (Fagan *et al.*, 1999b). We have also suggested the primary role of eNOS in regulating basal ID of the 100–1700 μm cat pulmonary arteries including muscular and elastic segments (Shirai *et al.*, 1999).

The present immunohistochemical analyses in the control rat have shown that eNOS-positive vessels were found in 91% of the elastic arteries >400 μm, but only in 9–51% of muscular arteries <300 μm (Table 3). This is consistent with the previous rat data that eNOS immunoreactivity is distributed among 96% of the pulmonary vessels (>150 μm ID), but only in 2–20% of the vessels smaller than this (Xue & Johns, 1996). The iNOS distribution data (Table 3) also agree with the previous data of very limited iNOS expression in vascular smooth muscle of all normoxic rat pulmonary arteries (Xue *et al.*, 1994; Xue & Johns, 1996; Cadogan *et al.*, 1999). We have further shown that in normoxic lungs, such eNOS and iNOS immunoreactivity distributions are almost in accord with the frequency distributions of ID constriction due to nonselective and iNOS selective inhibition, respectively (Figure 3).

Regional differences in vasodilator effect of endogenous NO in chronically hypoxic pulmonary arteries

It is generally agreed that main and extralobar pulmonary arteries isolated from CH rats have blunted endothelium-dependent relaxation to various receptor-dependent vasodilators (Crawley *et al.*, 1992; Rodman, 1992; Carville *et al.*, 1993; Shaul *et al.*, 1993; Maruyama & Maruyama, 1994) and to receptor-independent Ca^{2+} ionophore A-23187 (Carville *et al.*, 1993; Shaul *et al.*, 1993). However, different results have been obtained concerning whether CH alters the NO-mediated basal tone regulation in these proximal elastic pulmonary arteries. Some researchers have suggested that the effect of nonselective NOS inhibitor on basal tone is not significantly changed by CH (Rodman, 1992; Maruyama & Maruyama, 1994), whereas others have suggested its enhancement (Oka *et al.*, 1993). Moreover, basal NO production assessed by measuring cyclic guanosine-3′,5′-monophosphate (GMP) synthesis has been shown to decrease in main pulmonary arteries during chronic hypoxia (Shaul *et al.*, 1993). The present study showed that, in the transitional elastic arteries (400–500 μm), the nonselective NOS inhibitor-induced ID reduction is slightly but significantly larger in the CH rat than in the control rat, although no significant difference is present in the classical elastic arteries (600–700 μm) (Figure 2). In addition, the frequency distribution of ID response showed that the CH distribution curve is located slightly on the more constrictor side than the control curve in the transitional arteries, whereas no clear difference exists between these curves in the classical arteries (Figure 3). These results suggest that within the intralobar elastic arteries, small but significant degree of an enhancement of the NO-mediated basal vascular tone regulation is caused locally in the most distal vascular segment.

In the muscular pulmonary arteries (100–300 μm ID), there has been no direct observation on the change in NO-mediated control of basal vascular tone in response to CH. The present study has for the first time supplied information on the muscular arteries that the ID reduction due to nonselective NOS inhibition is significantly larger in the CH rat than in the control rat (Figure 2). Frequency distribution of ID response due to nonselective NOS inhibition showed that the CH distribution curve is located extremely on the more constrictor side than the control curve. Moreover, significant constriction was almost all ID responses in the CH vessels, but about half in the control vessels (Figure 3). These ID response patterns suggest that an increase in NO-mediated suppression of basal vascular tone occurs in most branches of the muscular arteries during CH, and probably explain the previous findings (Barer *et al.*, 1993; Oka *et al.*, 1993; Isaacson *et al.*, 1994; Roos *et al.*, 1996) that nonselective NOS inhibitor increased calculated resistance more greatly in perfused lungs obtained from CH rats than in those from normoxic rats.

It has recently been shown that iNOS inhibition with L-N^6-(1-iminoethyl)lysine dihydrochloride does not alter the dose–response change in calculated pulmonary arterial and venous resistance due to U-46619 in isolated, saline-perfused lungs from CH rats (Resta *et al.*, 1999). Moreover, this inhibition had no significant effect on PAP, SAP, and cardiac output in conscious hypoxic rats. From these data, they concluded that NO derived from iNOS does not modulate pulmonary vasoconstrictor responsiveness during CH (Resta *et al.*, 1999). The present study similarly showed that during iNOS inhibition (with L-canavanine or *S*-methylisothiourea), PAP and SAP did not significantly change in the CH rat (Table 2). However, we simultaneously found that there were significant ID reductions mainly in the muscular pulmonary arteries (Figure 2). Moreover, the frequency distribution of the ID response during iNOS inhibition showed that the CH distribution curve is located on the more constrictor side than the control curve in the muscular arteries, but, about half of the CH muscular arteries still exhibited no change, in contrast to the case of nonselective NOS inhibition (Figure 3). Therefore, for the same possible reason (local redistributions of flow from constricted to nonconstricted arteries) as mentioned above in the heterogenous vasoconstrictor effect of nonselective NOS inhibition on normoxic rats, we suppose that such a coexistence of ID constriction and no change in the parallel-arranged arteries during iNOS inhibition is also difficult to detect from changes in the pulmonary pressure–flow relation.

Previous studies have shown that in 2–4-week hypoxic rats, NOS immunoreactivity became markedly positive in the endothelial cells of most 80–150 μm pulmonary arteries

compared with normoxic rats (Xue *et al.*, 1994) and that the percentages (~95%) of eNOS-positive pulmonary vessels >150 μm ID are similar in 0–7-day hypoxic rats (Xue & Johns, 1996). Our findings that the percentages of eNOS-positive muscular arteries greatly rose up to 89–94% in the 4-week hypoxic lung, but those for elastic arteries displayed a slight increase (Table 3), support the previous data. However, we also provided new information that the eNOS distribution change corresponds well to the hypoxic change in the distribution of nonselective NOS inhibitor-induced ID reduction (Figure 3). On the other hand, iNOS protein has been shown to increase in the vascular smooth muscle of both muscular and elastic arteries obtained from CH rats (Xue *et al.*, 1994; Xue & Johns, 1996). For the first time, we found that 4-week hypoxia increases iNOS immunoreactivity scatteringly among the muscular and elastic arteries (Figure 5 and Table 3). The iNOS distribution in the muscular arteries was in accord with the distribution of iNOS inhibitor-induced ID reduction in these arteries (Figure 3). However, the increase in iNOS expression in the elastic arteries seems to be inconsistent with the data showing no significant effect of iNOS selective inhibition and no enhancement of nonselective NOS inhibitor effect in these arteries (Figures 2 and 3). The reason for this discrepancy remains to be elucidated. However, it has been shown that CH increases cyclic GMP phosphodiesterase activity in the larger intrapulmonary elastic arteries in the rat, but does not change it in the muscular arteries (MacLean *et al.*, 1997). It is therefore possible that in the elastic arteries, increased production of NO from iNOS cannot rise cyclic GMP level due to an increase in activity of cyclic GMP phosphodiesterase enzymes which catalyse cyclic GMP hydrolysis, while it can increase cyclic GMP level in the muscular arteries.

Together with the present finding of no significant ID response to nNOS inhibition, we conclude that in CH rats, both vasodilator effects of eNOS- and iNOS-derived NO are enhanced primarily in the muscular pulmonary arteries (100–300 μm); the enhancement of eNOS effects is induced extensively in these arteries, while that for iNOS sporadically in them. This is consistent with the previous data (Steudel *et al.*, 1998; Fagan *et al.*, 1999a, b) of marked pulmonary hypertension in eNOS-deficient mice raised in chronic hypoxia when compared with wild type, and suggests that NO production by eNOS is vital to counterbalance hypoxic pulmonary vasoconstriction, which is localized in muscular arteries (Shirai *et al.*, 1986; 1997; Barnes & Liu, 1995; Weir & Archer, 1995) and serves to inhibit the progress of pulmonary hypertension.

Possible factors responsible for nonuniform iNOS increase in hypoxic pulmonary arteries

iNOS was expressed in about half of the muscular pulmonary arteries of the chronic hypoxic rat, while eNOS in almost all these vessels (Table 3). It has been suggested that in the rat, the increase in eNOS expression after chronic hypoxia is due to the direct effect of hypoxia or hypoxia-induced factors independently of changes in haemodynamics (Everett *et al.*, 1998; Le Cras *et al.*, 1998). Therefore, it is possible that during chronic hypoxia, almost all muscular pulmonary arteries were exposed to low oxygen tension and, in turn, the upregulation of eNOS was induced in these arteries. On the other hand, the increase in iNOS expression may be caused by flow/wall shear stress (Rairigh *et al.*, 1999; Gosgnach *et al.*, 2000). We have previously shown that during acute inhalation of 5% O_2, ~60% of branches constrict in 100–200 μm feline muscular pulmonary arteries, but others display no significant response (Shirai *et al.*, 1986), meaning that hypoxia does not result in uniformly distributed pulmonary vasoconstriction. Acute hypoxia has also been shown to increase the heterogeneity of pulmonary vascular transit times throughout dog lung lobe (Dawson *et al.*, 1983). Moreover, chronic hypoxia at high altitude has been suggested to induce inhomogenous pulmonary vasoconstriction and regional overperfusion (Richalet, 1995; Hultgren, 1996; Bartsch, 1997). Such heterogenous distribution of vasoconstriction and blood flow may regionally increase shear stress and damage vascular endothelium (Richalet, 1995; West *et al.*, 1995; Bartsch, 1997; Botney, 1999). Indeed, endothelial injury with swelling in small peripheral arteries was observed in chronically hypoxic rats (Meyrick & Reid, 1978). Thus, we suggest a possibility that the heterogenous shear force distribution induced the vascular smooth muscle iNOS expression sporadically among the muscular pulmonary arteries (Figure 5 and Table 3) through the release of inflammatory mediators such as cytokines and eicosanoids and adhesion molecules (Richalet, 1995; Bartsch, 1997; Schoene *et al.*, 1988; Hansson *et al.*, 1994; Kubo *et al.*, 1996; Rabinovitch, 1997) and/or oxidative stress-induced NF-κ B activation after endothelial damage (Gosgnach *et al.*, 2000).

In conclusion, we suggest that, in 4-week hypoxia rats, functional and histological upregulation of eNOS and iNOS occurs chiefly in the muscular segments of pulmonary arteries. The eNOS upregulation is induced extensively in the muscular arteries, but the iNOS upregulation sporadically among these arteries. nNOS has no significant vasodilator effect. Such eNOS and iNOS upregulation may contribute to attenuating hypoxic pulmonary vasoconstriction which is localized in the muscular segments and, in turn, inhibit the progress of pulmonary hypertension.

This study was supported, in part, by a grant for the 'Ground Research for Space Utilization' promoted by NASDA and the Japan Space Forum; by Grants-in-Aid for Scientific Research from the Ministry of Education, Culture, Sports, Science, and Technology; by the Promotion of Fundamental studies in Health Science of the Organization for Pharmacological Safety and Research (OPSR); and by Health Sciences Grants (Funds for Human Genome Research and Regeneration Medicine Research, Japan.

References

ABRAHAM, A.S., KAY, J.M., COLE, R.B. & PINCOCK, A.C. (1971). Haemodynamic and pathological study of the effect of chronic hypoxia and subsequent recovery of the heart and pulmonary vasculature of the rat. *Cardiovasc. Res.*, 5, 95–102.

ADNOT, S., RAFFESTIN, B., EDDAHIBI, S., BRAQUET, P. & CHABRIER, P.-E. (1991). Loss of endothelium-dependent relaxant activity in the pulmonary circulation of rats exposed to chronic hypoxia. *J. Clin. Invest.*, 87, 155–162.

ALBERTINI, M., VANELLI, G. & CLEMENT, G. (1996). PGI_2 and nitric oxide involvement in the regulation of systemic and pulmonary basal vascular tone in the pig. *Prostaglandins Leukotr. Essent. Fatty Acids*, **54**, 273–278.

BARER, G., EMERY, C., STEWART, A., BEE, D. & HOWARD, P. (1993). Endothelial control of the pulmonary circulation in normal and chronically hypoxic rats. *J. Physiol.*, **463**, 1–16.

BARNARD, J.W., WILSON, P.S., MOORE, T.M., THOMPSON, W.J. & TAYLOR, A.E. (1993). Effect of nitric oxide and cyclooxygenase products on vascular resistance in dog and rat lungs. *J. Appl. Physiol.*, **74**, 2940–2948.

BARNES, P.J. & LIU, S.F. (1995). Regulation of pulmonary vascular tone. *Pharmacol. Rev.*, **47**, 87–131.

BARTSCH, P. (1997). High altitude pulmonary edema. *Respiration*, **64**, 435–443.

BEVAN, J.A. & LAHER, I. (1991). Pressure and flow-dependent vascular tone. *FASEB J.*, **5**, 2267–2273.

BOTNEY, M.D. (1999). Role of hemodynamics in pulmonary vascular remodeling. *Am. J. Respir. Crit. Care Med.*, **159**, 361–364.

CADOGAN, E., HOPKINS, N., GILES, S., BANNIGAN, J.G., MOYNIHAN, J. & MCLOUGHLIN, P. (1999). Enhanced expression of inducible nitric oxide synthase without vasodilator effect in chronically infected lungs. *Am. J. Physiol.*, **277**, L616–L627.

CARVILLE, C., RAFFESTIN, B., EDDAHIBI, S., BLOUQUIT, Y. & ADNOT, S. (1993). Loss of endothelium-dependent relaxation in proximal pulmonary arteries from rats exposed to chronic hypoxia: effects of *in vivo* and *in vitro* supplementation with L-arginine. *J. Cardiovasc. Pharmacol.*, **22**, 889–896.

CRAWLEY, D.E., ZHAO, L., GIEMBYCZ, M.A. & LIU, S. (1992). Chronic hypoxia impairs soluble guanylyl cyclase-mediated pulmonary arterial relaxation in the rat. *Am. J. Physiol.*, **263**, L325–L332.

CREMONA, G., WOOD, A.M., HALL, L.W., BOWER, E.A. & HIGENBOTTAM, T. (1994). Effect of inhibitors of nitric oxide release and action on vascular tone in isolated lungs of pig, sheep, dog and man. *J. Physiol.*, **481**, 185–195.

DAWSON, C.A., BRONIKOWSKI, T.A., LINEHAN, J.H. & HAKIM, T.S. (1983). Influence of pulmonary vasoconstriction on ling water and perfusion heterogeneity. *J. Appl. Physiol.*, **54**, 654–660.

EDDAHIBI, S., ADNOT, S., CARVILLE, C., BLOUQUIT, Y. & RAFFESTIN, B. (1992). L-Arginine restores endothelium-dependent relaxation in pulmonary circulation of chronically hypoxic rats. *Am. J. Physiol.*, **263**, L194–L200.

EVERETT, A.D., LE CRAS, T.D., XUE, C. & JOHNS, R.A. (1998). eNOS expression is not altered in pulmonary vascular remodeling due to increased pulmonary blood flow. *Am. J. Physiol.*, **274**, L1058–L1065.

FAGAN, K.A., FOUTY, B.W., TYLER, R.C., MORRIS JR, K.G., HEPLER, L.K., SATO, K., LE CRAS, T.D., ABMAN, S.H., WEINBERGER, H.D., HUANG, P.L., MCMURTRY, I.F. & RODMAN, D.M. (1999a). The pulmonary circulation of homozygous or heterozygous eNOS-null mice is hyperresponsive to mild hypoxia. *J. Clin. Invest.*, **103**, 291–299.

FAGAN, K.A., TYLER, R.C., SATO, K, FOUTY, B.W., Morris JR, K.G., HUANG, P.L., MCMURTRY, I.F. & RODMAN, D.M. (1999b). Relative contributions of endothelial, inducible, and neuronal NOS to tone in the murine pulmonary circulation. *Am. J. Physiol.*, **277**, L472–L478.

FINEMAN, J.R., HEYMANN, M.A. & SOIFER, S.J. (1991). N^{ω}-nitro-L-arginine attenuates endothelium-dependent pulmonary vasodilation in lambs. *Am. J. Physiol.*, **260**, H1299–H1306.

GORDON, J.B. & TOD, M.L. (1993). Effects of N^{ω}-nitro-L-arginine on total and segmental vascular resistances in developing lamb lungs. *J. Appl. Physiol.*, **75**, 76–85.

GOSGNACH, W., MESSIKA-ZEITOUN, D., GONZALEZ, W., PHILIPE, M. & MICHEL, J.-B. (2000). Shear stress induces iNOS expression in cultured smooth muscle cells: roles of oxidative stress. *Am. J. Physiol.*, **279**, C1880–C1888.

HAKIM, T.S. (1994). Flow-induced release of EDRF in the pulmonary vasculature: site of release and action. *Am. J. Physiol.*, **267**, H363–H369.

HAMPL, V., ARCHER, S.L., NELSON, D.P. & WEIR, E.K. (1993). Chronic EDRF inhibition and hypoxia: effects on pulmonary circulation and systemic blood pressure. *J. Appl. Physiol.*, **75**, 1748–1757.

HANSSON, G.K., GENG, Y.-J., HOLM, J., HARDHAMMAR, P., WENNMALM, A. & JENNISCHE, E. (1994). Arterial smooth muscle cells express nitric oxide synthase in response to endothelial injury. *J. Exp. Med.*, **180**, 733–738.

HASUNUMA, K., YAMAGUCHI, T., RODMAN, D.M., O'BRIEN, R.F. & MCMURTRY, I.F. (1991). Effects of inhibitors of EDRF and EDHF on vasoreactivity of perfused rat lungs. *Am. J. Physiol.*, **260**, L97–L104.

HUANG, M., LEBLANC, M.L. & HESTER, R.L. (1994). Systemic and regional hemodynamics after nitric oxide synthase inhibition: role of a neurogenic mechanism. *Am. J. Physiol.*, **267**, R84–R88.

HULTGREN, H.N. (1996). High-altitude pulmonary edema: current concepts. *Annu. Rev. Med.*, **47**, 267–284.

ISAACSON, T.C., HAMPL, V., WEIR, E.K., NELSON, D.P. & ARCHER, S.L. (1994). Increased endothelium-derived NO in hypertensive pulmonary circulation of chronically hypoxic rats. *J. Appl. Physiol.*, **76**, 933–940.

KALISCH, B.E., CONNOP, B.P., JHAMANDAS, K., BENINGER, R.J. & BOEGMAN, R.J. (1996). Differential action of 7-nitro indazole on rat brain nitric oxide synthase. *Neurosci. Lett.*, **219**, 75–78.

KAY, J.M. (1983). Pulmonary vasculature and nerves. Comparative morphologic features of the pulmonary vasculature in mammals. *Am. Rev. Respir. Dis.*, **128**, S53–S57.

KUBO, K, HANAOKA, M., YAMAGUCHI, S., HAYANO, T., HAYASAKA, M., KOIZUMI, T., FUJIMOTO, K., KOBAYASHI, T. & HONDA, T. (1996). Cytokines in bronchoalveolar lavage fluid in patients with high altitude pulmonary oedema at moderate altitude in Japan. *Thorax*, **51**, 739–742.

LE CRAS, T.D., TYLER, R.C., HORAN, M.P., MORRIS, K.G., TUDER, R.M. & MCMURTRY, I.F. (1998). Effects of chronic hypoxia and altered hemodynamics on endothelial nitric oxide synthase expression in the adult rat lung. *J. Clin. Invest.*, **101**, 795–801.

LE CRAS, T.D., XUE, C., RENGASAMY, A. & JOHNS, R.A. (1996). Chronic hypoxia upregulates endothelial and inducible NO synthase gene and protein expression in rat lung. *Am. J. Physiol.*, **270**, L164–L170.

LEEMAN, M., ZEGERS DE BEYL, V., DELCROIX, M. & NAEIJE, R. (1994). Effects of endogenous nitric oxide on pulmonary vascular tone in intact dogs. *Am. J. Physiol.*, **266**, H2343–H2347.

LIAUDET, L., FEIHL, F., ROSSELET, A., MARKERT, M., HURNI, J.-M. & PERRET, C. (1996). Beneficial effects of L-canavanine, a selective inhibitor of inducible nitric oxide synthase, during rodent endotoxaemia. *Clin. Sci.*, **90**, 369–377.

LOEB, A.L. & LONGNECKER, D.E. (1992). Inhibition of endothelium-derived relaxing factor-dependent circulatory control in intact rats. *Am. J. Physiol.*, **262**, H1494–H1500.

MACLEAN, M.R., JOHNSTON, E.D., MCCULLOCH, K.M., POOLEY, L., HOUSLAY, M.D. & SWEENEY, G. (1997). Phosphodiesterase isoforms in the pulmonary arterial circulation of the rat: changes in pulmonary hypertension. *J. Pharmacol. Exp. Ther.*, **283**, 619–624.

MARUYAMA, J. & MARUYAMA, K. (1994). Impaired nitric oxide-dependent responses and their recovery in hypertensive pulmonary arteries of rats. *Am. J. Physiol.*, **266**, H2476–H2488.

MCCORMACK, D.G. & PATERSON, N.A.M. (1993). Loss of hypoxic pulmonary vasoconstriction in chronic pneumonia is not mediated by nitric oxide. *Am. J. Physiol.*, **265**, H1523–H1528.

MCMAHON, T.J., HOOD, J.S., BELLAN, J.A. & KADOWITZ, P.J. (1991). N^{ω}-nitro-L-arginine methyl ester selectively inhibits pulmonary vasodilator responses to acetylcholine and bradykinin. *J. Appl. Physiol.*, **71**, 2026–2031.

MEYRICK, B. & REID, L. (1978). The effect of continued hypoxia on rat pulmonary arterial circulation. An ultrastructural study. *Lab. Invest.*, **38**, 188–200.

MOORE, P.K., WALLACE, P., GAFFEN, Z., HART, S.L. & BABBEDGE, R.C. (1993). Characterization of the novel nitric oxide synthase inhibitor 7-nitro indazole and related indazoles: antinociceptive and cardiovascular effects. *Br. J. Pharmacol.*, **110**, 219–224.

MURAMATSU, M., RODMAN, D.M., OKA, M. & MCMURTRY, I.F. (1996). Thapsigargin stimulates NO activity in hypoxic hypertensive rat lungs and pulmonary arteries. *J. Appl. Physiol.*, **80**, 1336–1344.

MURAMATSU, M., RODMAN, D.M., OKA, M. & MCMURTRY, I.F. (1997). Endothelin-1 mediates nitro-L-arginine vasoconstriction of hypertensive rat lungs. *Am. J. Physiol.*, **272**, L807–L812.

NELIN, L.D. & DAWSON, C.A. (1993). The effect of N^{ω}-nitro-L-arginine methyl ester on hypoxic vasoconstriction in the neonatal pig lung. *Pediatr. Res.*, **34**, 349–353.

NISHIWAKI, K., NYHAN, D.P., ROCK, P., DESAI, P.M., PETERSON, W.P., PRIBBLE, C.G. & MURRAY, A. (1992). N^{ω}-nitro-L-arginine and pulmonary vascular pressure–flow relationship in conscious dogs. *Am. J. Physiol.*, **262**, H1331–H1337.

OKA, M., HASUNUMA, K., WEBB, S.A., STELZNER, T.J., RODMAN, D.M. & MCMURTRY, I.F. (1993). EDRF suppresses an unidentified vasoconstrictor mechanism in hypertensive rat lungs. *Am. J. Physiol.*, **264**, L587–L597.

OKAMOTO, H., HUDETZ, A.G., ROMAN, R.J., BOSNJAK, Z.J. & KAMPINE, J.P. (1997). Neuronal NOS-derived NO plays permissive role in cerebral blood flow response to hypercapnia. *Am. J. Physiol.*, **272**, H559–H566.

PERSSON, M.G., GUSTAFSSON, L.E., WIKLUND, N.P., MONCADA, S. & HEDQVIST, P. (1990). Endogenous nitric oxide as a probable modulator of pulmonary circulation and hypoxic pressor response *in vivo*. *Acta Physiol. Scand.*, **140**, 449–457.

RABINOVITCH, M. (1997). Pulmonary hypertension: updating a mysterious disease. *Cardiovasc. Res.*, **34**, 268–272.

RABINOVITCH, M., GAMBLE, W., NADAS, A.S., MIETTINEN, O.S. & REID, L. (1979). Rat pulmonary circulation after chronic hypoxia: hemodynamic and structural features. *Am. J. Physiol.*, **236**, H818–H827.

RAIRIGH, R.L., STORME, L., PARKER, T.A., LE CRAS, T.D., KINSELLA, J.P., JAKKULA, M. & ABMAN, S.H. (1999). Inducible NO synthase inhibition attenuates shear stress-induced pulmonary vasodilation in the ovine fetus. *Am. J. Physiol.*, **276**, L513–L521.

RESTA, T.C., GONZALES, R.J., DAIL, W.G., SANDERS, T.C. & WALKER, B.R. (1997). Selective upregulation of arterial endothelial nitric oxide synthase in pulmonary hypertension. *Am. J. Physiol.*, **272**, H806–H813.

RESTA, T.C., O'DONAUGHY, T.L., EARLEY, S., CHICOINE, L.G. & WALKER, B.R. (1999). Unaltered vasoconstrictor responsiveness after iNOS inhibition in lungs from chronically hypoxic rats. *Am. J. Physiol.*, **276**, L122–L130.

RESTA, T.C. & WALKER, B.R. (1996). Chronic hypoxia selectively augments endothelium-dependent pulmonary arterial vasodilation. *Am. J. Physiol.*, **270**, H888–H896.

RICHALET, J.-P. (1995). High altitude pulmonary oedema: still a place for controversy? *Thorax*, **50**, 923–929.

ROBERTSON, B.E., WARREN, J.B. & NYE, P.C.G. (1990). Inhibition of nitric oxide synthesis potentiates hypoxic vasoconstriction in isolated rat lungs. *Exp. Physiol.*, **75**, 255–257.

RODMAN, D.M. (1992). Chronic hypoxia selectively augments rat pulmonary artery Ca^{2+} and K^{+} channel-mediated relaxation. *Am. J. Physiol.*, **263**, L88–L94.

ROOS, C.M., FRANK, D.U., XUE, C., JOHNS, R.A. & RICH, G.F. (1996). Chronic inhaled nitric oxide: effects on pulmonary vascular endothelial function and pathology in rats. *J. Appl. Physiol.*, **80**, 252–260.

RUSS, R.D. & WALKER, B.R. (1993). Maintained endothelium-dependent pulmonary vasodilation following chronic hypoxia in the rat. *J. Appl. Physiol.*, **74**, 339–344.

SADA, K., SHIRAI, M. & NINOMIYA, I. (1985). X-ray TV system for measuring microcirculation in small pulmonary vessels. *J. Appl. Physiol.*, **59**, 1013–1018.

SASAKI, S.-I., KOBAYASHI, N., DAMBARA, T., KIRA, S. & SAKAI, T. (1995). Structural organization of pulmonary arteries in the rat lung. *Anat. Embryol.*, **191**, 477–489.

SCHOENE, R.B., SWENSON, E.R., PIZZO, C.J., HACKETT, P.H., ROACH, R.C., MILLS JR, W.J., HENDERSON JR, W.R. & MARTIN, T.R. (1988). The lung at high altitude: bronchoalveolar lavage in acute mountain sickness and pulmonary edema. *J. Appl. Physiol.*, **64**, 2605–2613.

SHAUL, P.W., NORTH, A.J., BRANNON, T.S., UJIIE, K., WELLS, L.B., NISEN, P.A., LOWENSTEIN, C.J., SNYDER, S.H. & STAR, R.A. (1995). Prolonged *in vivo* hypoxia enhances nitric oxide synthase type I and type III gene expression in adult rat lung. *Am. J. Respir. Cell Mol. Biol.*, **13**, 167–174.

SHAUL, P.W., WELLS, L.B. & HORNING, K.M. (1993). Acute and prolonged hypoxia attenuates endothelial nitric oxide production in rats pulmonary arteries by different mechanisms. *J. Cardiovasc. Pharmacol.*, **22**, 819–827.

SHIRAI, M., IKEDA, S., MIN, K.-Y., SHIMOUCHI, A., KAWAGUCHI, A.T. & NINOMIYA, I. (1999). Segmental differences in vasodilatation due to basal NO release in *in vivo* cat pulmonary vessels. *Respir. Physiol.*, **116**, 159–169.

SHIRAI, M., SADA, K. & NINOMIYA, I. (1986). Effects of regional alveolar hypoxia and hypercapnia on small pulmonary vessels in cats. *J. Appl. Physiol.*, **61**, 440–448.

SHIRAI, M., SHIMOUCHI, A., KAWAGUCHI, A.T., IKEDA, S., SUNAGAWA, K. & NINOMIYA, I. (1997). Endogenous nitric oxide attenuates hypoxic pulmonary vasoconstriction of small pulmonary arteries and veins in anaesthetized cats. *Acta Physiol. Scand.*, **159**, 263–264.

SPRAGUE, R.S., STEPHENSON, A.H., DIMMITT, R.A., WEINTRAUB, N.A., BRANCH, L., MCMURDO, L. & LONIGRO, A.J. (1995). Effect of L-NAME on pressure–flow relationships in isolated rabbit lungs: role of red blood cells. *Am. J. Physiol.*, **269**, H1941–H1948.

STAMLER, J.S., LOH, E., RODDY, M.-A., CURRIE, K.E. & CREAGER, M.A. (1994). Nitric oxide regulates basal systemic and pulmonary vascular resistance in healthy humans. *Circulation*, **89**, 2035–2040.

STEUDEL, W., ICHINOSE, F., HUANG, P.L., HURFORD, W.E., JONES, R.C., BEVAN, J.A., FISHMAN, M.C. & ZAPOL, W.M. (1997). Pulmonary vasoconstriction and hypertension in mice with targeted disruption of the endothelial nitric oxide synthase (NOS 3) gene. *Circ. Res.*, **81**, 34–41.

STEUDEL, W., SCHERRER-CROSBIE, M., BLOCH, K.D., WEIMANN, J., HUANG, P.L., JONES, R.C., PICARD, M.H. & ZAPOL, W.M. (1998). Sustained pulmonary hypertension and right ventricular hypertrophy after chronic hypoxia in mice with congenital deficiency of nitric oxide synthase 3. *J. Clin. Invest.*, **101**, 2468–2477.

SZABO, C., SOUTHAN, G.J. & THIEMERMANN, C. (1994). Beneficial effects and improved survival in rodent models of septic shock with *S*-methylisothiourea sulfate, a potent and selective inhibitor of inducible nitric oxide synthase. *Proc. Natl. Acad. Sci. U.S.A.*, **91**, 12472–12476.

TEALE, D.M. & ATKINSON, A.M. (1994). L-Canavanine restores blood pressure in a rat model of endotoxin shock. *Eur. J. Pharmacol.*, **271**, 87–92.

TYLER, R.C., MURAMATSU, M., ABMAN, S.H., STELZNER, T.J., RODMAN, D.M., BLOCH, K.D. & MCMURTRY, I.F. (1999). Variable expression of endothelial NO synthase in three forms of rat pulmonary hypertension. *Am. J. Physiol.*, **276**, L297–L303.

UMANS, J.G. (1995). Nitric oxide in the regulation of blood flow and arterial pressure. *Annu. Rev. Physiol.*, **57**, 771–790.

WEIR, E.K. & ARCHER, S. (1995). The mechanism of acute hypoxic pulmonary vasoconstriction: the tale of two channels. *FASEB J.*, **9**, 183–189.

WEST, J.B., COLICE, G.L., LEE, Y.-J., NAMBA, Y., KURDAK, S.S., FU, Z., OU, L.C. & MATHIEU-COSTELLO, O. (1995). Pathogenesis of high-altitude pulmonary oedema: direct evidence of stress failure of pulmonary capillaries. *Eur. Respir. J.*, **8**, 523–529.

XUE, C. & JOHNS, R.A. (1996). Upregulation of nitric oxide synthase correlates temporally with onset of pulmonary vascular remodeling in the hypoxic rat. *Hypertension*, **28**, 743–753.

XUE, C., RENGASAMY, A., LE CRAS, T.D., KOBERNA, P.A., DAILEY, G.C. & JOHNS, R.A. (1994). Distribution of NOS in normoxic vs hypoxic rat lung: upregulation of NOS by chronic hypoxia. *Am. J. Physiol.*, **267**, L667–L678.

(Received December 2, 2002
Revised March 3, 2003
Accepted April 7, 2003)

Am J Physiol Heart Circ Physiol 285: H2125–H2131, 2003;
10.1152/ajpheart.00548.2002.

Repeated inhalation of adrenomedullin ameliorates pulmonary hypertension and survival in monocrotaline rats

Noritoshi Nagaya,[1] Hiroyuki Okumura,[2] Masaaki Uematsu,[3] Wataru Shimizu,[1] Fumiaki Ono,[1] Mikiyasu Shirai,[4] Hidezo Mori,[4] Kunio Miyatake,[1] and Kenji Kangawa[2]

[1]*Department of Internal Medicine, National Cardiovascular Center, Osaka 565-8565;*
[2]*Department of Biochemistry, National Cardiovascular Center Research Institute, Osaka 565-8565;*
[3]*Cardiovascular Division, Kansai Rosai Hospital, Hyogo 660-0064, Japan; and* [4]*Department of Cardiac Physiology, National Cardiovascular Center Research Institute, Osaka, Japan 565-8565*

Submitted 1 July 2002; accepted in final form 31 December 2002

Nagaya, Noritoshi, Hiroyuki Okumura, Masaaki Uematsu, Wataru Shimizu, Fumiaki Ono, Mikiyasu Shirai, Hidezo Mori, Kunio Miyatake, and Kenji Kangawa. Repeated inhalation of adrenomedullin ameliorates pulmonary hypertension and survival in monocrotaline rats. *Am J Physiol Heart Circ Physiol* 285: H2125–H2131, 2003; 10.1152/ajpheart.00548.2002.—Adrenomedullin (AM) is a potent vasodilator peptide. We investigated whether inhalation of aerosolized AM ameliorates monocrotaline (MCT)-induced pulmonary hypertension in rats. Male Wistar rats given MCT (MCT rats) were assigned to receive repeated inhalation of AM ($n = 8$) or 0.9% saline ($n = 8$). AM (5 μg/kg) or saline was inhaled as an aerosol using an ultrasonic nebulizer for 30 min four times a day. After 3 wk of inhalation therapy, mean pulmonary arterial pressure and total pulmonary resistance were markedly lower in rats treated with AM than in those given saline [mean pulmonary arterial pressure: 22 ± 2 vs. 35 ± 1 mmHg (−37%); total pulmonary resistance: 0.048 ± 0.004 vs. 0.104 ± 0.006 mmHg·ml^{-1}·min^{-1}·kg^{-1} (−54%), both $P < 0.01$]. Neither systemic arterial pressure nor heart rate was altered. Inhalation of AM significantly attenuated the increase in medial wall thickness of peripheral pulmonary arteries in MCT rats. Kaplan-Meier survival curves demonstrated that MCT rats treated with aerosolized AM had a significantly higher survival rate than those given saline (70% vs. 10% 6-wk survival, log-rank test, $P < 0.01$). In conclusion, repeated inhalation of AM inhibited MCT-induced pulmonary hypertension without systemic hypotension and thereby improved survival in MCT rats.

vasodilator; hemodynamics; aerosol; survival

ADRENOMEDULLIN (AM) is a potent vasodilator peptide that was originally isolated from human pheochromocytoma (13). Immunoreactive AM has subsequently been detected in plasma and a variety of tissues, including blood vessels and the lungs (9, 27). It has been reported that there are abundant binding sites for AM in the lungs (24). We (11, 30) have shown that the plasma AM level increases in proportion to the severity of pulmonary hypertension and that circulating AM is partially metabolized in the lungs. Interestingly, AM has been shown to inhibit the migration and proliferation of vascular smooth muscle cells (8, 12). These findings suggest that AM plays an important role in the regulation of pulmonary vascular tone and vascular remodeling.

In fact, experimental studies (5, 14, 22) have demonstrated that intralobar arterial infusion of AM induces pulmonary vasodilation in rats and cats. In humans, we have shown that short-term intravenous infusion of AM significantly decreases pulmonary vascular resistance in patients with congestive heart failure (19) or primary pulmonary hypertension (PPH) (18). Unfortunately, however, intravenously administered AM also decreases systemic arterial pressure in such patients because of its nonselective vasodilation in pulmonary and systemic vascular beds.

Recently, inhaled prostacyclin and its analog, iloprost, have been shown to cause pulmonary vasodilation without systemic hypotension in patients with PPH (7, 28, 29). In addition, the inhalant application of vasodilators does not induce negative side effects on gas exchange, because ventilation-matched deposition of the drugs in the alveoli causes pulmonary vasodilation matched to ventilated areas (28). In clinical settings, inhalation therapy may be more simple, noninvasive, and relatively comfortable than continuous intravenous infusion therapy. These findings raise the possibility that intratracheal delivery of aerosolized AM may have beneficial effects in patients with precapillary pulmonary hypertension.

Thus the purpose of the present study was to investigate whether inhalation of AM ameliorates monocrotaline (MCT)-induced pulmonary hypertension and thereby improves survival in MCT-treated rats.

METHODS

Animals. Male Wistar rats weighing 80 to 100 g were used in this study. The rats were given a subcutaneous injection of 60 mg/kg MCT (MCT rats) and assigned to receive a single inhalation of AM ($n = 5$) or 0.9% saline ($n = 5$) or repeated inhalation of AM ($n = 8$) or 0.9% saline ($n = 8$). Sham rats not

Address for reprint requests and other correspondence: N. Nagaya, Dept. of Internal Medicine, National Cardiovascular Center, 5-7-1 Fujishirodai, Suita, Osaka 565-8565, Japan (E-mail: nagayann@hsp.ncvc.go.jp).

The costs of publication of this article were defrayed in part by the payment of page charges. The article must therefore be hereby marked "*advertisement*" in accordance with 18 U.S.C. Section 1734 solely to indicate this fact.

given a MCT injection also received repeated inhalation of AM ($n = 8$) or 0.9% saline ($n = 8$). An additional 20 rats were studied to evaluate the effects of inhaled AM on survival in MCT rats. Finally, rats that had developed pulmonary hypertension 3 wk after the MCT injection received repeated inhalation of AM ($n = 8$) or 0.9% saline ($n = 8$). All protocols were performed in accordance with guidelines of the Animal Care Ethics Committee of the National Cardiovascular Center Research Institute (Osaka, Japan).

Preparation of AM. Recombinant human AM was obtained from Shionogi (Osaka, Japan). The homogeneity of AM was confirmed by reverse-phase HPLC and amino acid analysis. AM was dissolved in 0.9% saline, and the solution was stored as 20-ml volumes containing 200 μg AM/tube at −80°C until the time of preparation for administration.

Inhalation of AM. We used an unrestrained, whole body aerosol exposure system. Each rat was placed in a plastic cage for aerosol delivery. AM or saline was aerosolized using an ultrasonic nebulizer (Soniclizer 305, Atom) connected to six cages. The 20 ml solution containing 200 μg AM was delivered as an aerosol into the six cages at a constant flow rate (0.6 ml solution/min) for 30 min. Inhalation of fluorescein isothiocyanate-dextran demonstrated that a single inhalation of AM delivered 0.5 μg AM to the lungs in each rat (5 μg/kg body wt).

To assess the acute effect of inhaled AM, hemodynamic studies were carried out at 3 wk after the MCT injection. Hemodynamics were measured at 15-min intervals before, during, and after a single inhalation of AM or saline. Blood was obtained from the carotid artery at the same time points for measurement of plasma AM.

To assess the chronic effect of inhaled AM, 30-min inhalation of AM (5 μg/kg body wt) or saline was repeated four times a day for 3 wk after the MCT injection. Finally, to investigate the effects of inhaled AM on developed pulmonary hypertension, aerosolized AM or saline was given for 1 wk to rats that had developed pulmonary hypertension 3 wk after the MCT injection. After completion of the inhalation therapy, hemodynamic studies were performed. Blood was then drawn from the carotid artery for measurement of plasma hormone levels. Finally, cardiac arrest was induced by the injection of 2 mmol KCl through the catheter. The ventricles and lungs were excised, dissected free, and weighed. The measurement of right ventricular weight excluded the interventricular septum. The ratio of right ventricular weight to body weight and the ratio of left ventricular weight to body weight were calculated as indexes of ventricular hypertrophy.

Hemodynamic measurements. Rats were anesthetized with intraperitoneal pentobarbital (30 mg/kg) and placed on a heating pad to maintain body temperature at 37–38°C throughout the study. A polyethylene catheter (PE-10) was inserted into the right femoral artery to measure heart rate and mean arterial pressure. An umbilical vessel catheter was inserted through the right jugular vein into the pulmonary artery for the measurement of right ventricular pressure and pulmonary arterial pressure. These hemodynamic variables were measured using a pressure transducer (model P23ID, Gould) connected to a polygraph and recorded with a thermal recorder (7758B system, Hewlett-Packard). A thermomicroprobe was advanced into the ascending aorta via the right carotid artery and connected to a cardiac output computer (Cardiotherm-500, Columbus Instruments). Cardiac output was measured in triplicate by the thermodilution method. Total pulmonary resistance was calculated by dividing the mean pulmonary arterial pressure by the cardiac output.

Morphometric analysis of pulmonary arteries. Paraffin sections 4 μm in thickness were obtained from the middle region of the right lung and stained with hematoxylin and eosin for examination by light microscopy. Analysis of the medial wall thickness of the pulmonary arteries was performed as described previously (23). In brief, the external diameter and the medial wall thickness were measured in 20 muscular arteries (ranging in external diameter from 25 to 50 and from 51 to 100 μm) per lung section. For each artery, the medial wall thickness was expressed as follows: percent wall thickness = [(medial thickness × 2)/external diameter] × 100. A lung section was obtained from individual rats for comparison among the four groups ($n = 5$ each).

Hormonal analysis. The plasma AM level was measured by an immunoradiometric assay using a specific kit (Shionogi) (22). For the assessment of right ventricular function (17, 21), the plasma atrial natriuretic peptide (ANP) level was measured using an enzyme immunoassay kit (ANF Rat EIA kit; Peninsula, CA).

Survival analysis. To evaluate the effects of inhaled AM on survival in MCT rats, 20 rats received repeated inhalation of AM ($n = 10$) or saline ($n = 10$) four times a day from the date of the MCT injection until death. Survival was estimated from the date of the MCT injection to the death of the rat or 6 wk after the injection.

Statistical analysis. All data are expressed as means ± SE unless otherwise indicated. Comparisons of parameters among three groups were made by one-way ANOVA, followed by Scheffé's multiple-comparison test. Comparisons of the time course of parameters between two groups were made by two-way ANOVA for repeated measures, followed by Scheffé's multiple-comparison test. Survival curves according to the presence or absence of AM inhalation were derived using the Kaplan-Meier method and compared using a log-rank test. A P value <0.05 was considered statistically significant.

RESULTS

Acute effect of single inhalation of AM. Acute hemodynamic studies were carried out at 3 wk after the MCT injection. AM inhalation slightly increased the circulating level of human AM (from 0 to 3.6 ± 1.0 fmol/ml, $P < 0.05$). A 30-min inhalation of AM slightly but significantly decreased the mean pulmonary arterial pressure in MCT rats (from 32 ± 2 to 29 ± 2 mmHg, $P < 0.05$; Fig. 1) without a significant decrease in mean arterial pressure (from 113 ± 5 to 111 ± 4 mmHg, P = not signficant). AM inhalation markedly increased cardiac output by 42% (from 405 ± 22 to 575 ± 34 $ml \cdot min^{-1} \cdot kg^{-1}$, $P < 0.05$) at the end of inhalation. Thus AM resulted in a 36% decrease in total pulmonary resistance (from 0.081 ± 0.006 to 0.052 ± 0.004 $mmHg \cdot ml^{-1} \cdot min^{-1} \cdot kg^{-1}$, $P < 0.05$). The ratio of total pulmonary resistance to systemic vascular resistance was significantly decreased at the end of inhalation (from 0.29 ± 0.01 to 0.26 ± 0.01, $P < 0.05$). Interestingly, these hemodynamic effects of AM lasted at least 60 min after the end of inhalation. Inhalation of saline did not alter any hemodynamic or hormonal parameter.

Chronic effect of repeated inhalation of AM. The physiological profiles of the four experimental groups are summarized in Table 1. Body weight was significantly lower in both MCT groups than in sham rats.

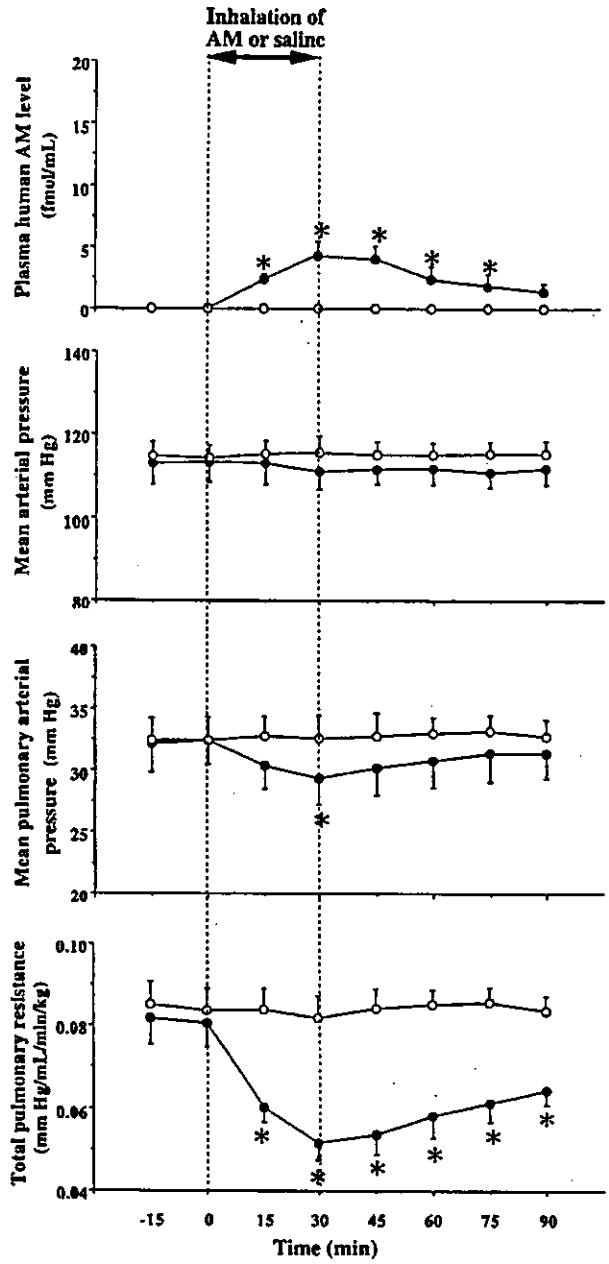

Fig. 1. Acute hemodynamic and hormonal responses to inhaled adrenomedullin (AM; ●) or saline (○) in monocrotaline (MCT)-treated rats (MCT rats). Data are means ± SE. *$P < 0.05$ vs. *time 0*.

Right ventricular weight was significantly lower in MCT rats receiving repeated inhalation of AM than in those given aerosolized saline. There was no significant difference in left ventricular weight among the four groups.

Three weeks after the MCT injection, pulmonary hypertension developed compared with findings in sham rats, but the rise in mean pulmonary arterial pressure was markedly attenuated in MCT rats treated with repeated inhalation of AM (by 37%) compared with that in MCT rats given aerosolized saline (22 ± 2 vs. 35 ± 1 mmHg, $P < 0.05$; Fig. 2). Cardiac output was significantly higher in MCT rats treated with AM (by 30%) compared with that in MCT rats given saline (444 ± 18 vs. 342 ± 18 $ml \cdot min^{-1} \cdot kg^{-1}$, $P < 0.05$). Therefore, total pulmonary resistance was markedly lower in MCT rats treated with AM (by 54%) compared with that in MCT rats given saline (0.048 ± 0.004 vs. 0.104 ± 0.006 $mmHg \cdot ml^{-1} \cdot min^{-1} \cdot kg^{-1}$, $P < 0.05$). Similarly, the increase in right ventricular systolic pressure was significantly attenuated by AM inhalation (Table 1). In contrast, neither mean arterial pressure nor heart rate differed among the four groups. The ratio of total pulmonary resistance to systemic vascular resistance was markedly lower in MCT rats treated with aerosolized AM (by 44%) compared with that in MCT rats given aerosolized saline (0.19 ± 0.01 vs. 0.34 ± 0.01, $P < 0.05$). Inhalation of AM did not significantly alter any hemodynamic parameters in sham rats.

Representative photomicrographs of pulmonary arteries showed that hypertrophy of the pulmonary vessel wall was inhibited in MCT rats treated with AM compared with that in MCT rats given saline (Fig. 3). Quantitative analysis of peripheral pulmonary arteries demonstrated that the percent wall thickness of pulmonary arteries was significantly lower in MCT rats treated with aerosolized AM than in those given aerosolized saline (20 ± 1% vs. 28 ± 1% in vasculature with an external diameter of 25–50 μm and 21 ± 1% vs. 27 ± 1% in vasculature with an external diameter of 51–100 μm, both $P < 0.05$; Fig. 3). Inhalation of AM did not significantly alter vascular morphology in sham rats.

Effect of AM inhalation on long-term prognosis in MCT rats. Kaplan-Meier survival curves demonstrated that MCT rats treated with aerosolized AM had a significantly higher survival rate than those given saline (70% vs. 10% in 6-wk survival, log-rank test, $P < 0.01$; Fig. 4). No definite adverse effects were detected after repeated inhalation of AM.

Effect of AM inhalation on developed pulmonary hypertension. AM or saline was inhaled by rats that had developed pulmonary hypertension 3 wk after the MCT injection. Mean pulmonary arterial pressure was significantly lower in MCT rats treated with AM (by 14%) compared with that in rats given saline (32 ± 1 vs. 37 ± 1 mmHg, $P < 0.05$). Cardiac output was also higher in MCT rats treated with AM (by 15%) compared with that in rats given saline (360 ± 11 vs. 313 ± 14 $ml \cdot min^{-1} \cdot kg^{-1}$, $P < 0.05$). Therefore, total pulmonary resistance was significantly lower in MCT rats treated with AM (by 24%) compared with that in rats given saline (0.091 ± 0.005 vs. 0.119 ± 0.008 $mmHg \cdot ml^{-1} \cdot min^{-1} \cdot kg^{-1}$, $P < 0.05$).

DISCUSSION

In the present study, we demonstrated that *1*) a single inhalation of AM using an ultrasonic nebulizer induced relatively long-lasting pulmonary vasodilation without systemic hypotension, *2*) repeated inhalation

Table 1. *Physiological profiles of the four experimental groups*

	Sham		MCT	
	Sham-Saline	Sham-AM	MCT-Saline	MCT-AM
n	8	8	8	8
Body weight, g	150±3	154±3	132±2*	146±4†
RV/body wt, g/kg	0.59±0.02	0.58±0.01	0.92±0.06*	0.66±0.02†
LV/body wt, g/kg	2.32±0.04	2.27±0.05	2.48±0.05	2.33±0.05
Heart rate, beats/min	409±15	428±20	424±15	413±14
Mean arterial pressure, mmHg	120±3	117±3	104±3*	115±3†
RV systolic pressure, mmHg	35±1	34±1	67±2*	45±3*†
Right atrial pressure, mmHg	2±1	2±1	7±1*	2±1†
Plasma ANP level, pg/ml	275±40	238±29	694±61*	346±44†

Values are means ± SE; *n*, number of rats. Sham-saline, sham rats given aerosolized saline; sham-AM, sham rats given aerosolized AM; MCT-saline, rats treated with monocrostaline (MCT) and given aerosolized saline; MCT-AM, rats treated with MCT and given aerosolized AM; RV, right ventricular LV, left ventricular; ANP, atrial natriuretic peptide. *$P < 0.05$ vs. sham-saline; †$P < 0.05$ vs. MCT-saline.

of AM ameliorated MCT-induced pulmonary hypertension and attenuated the development of pulmonary vascular remodeling, and 3) inhalation of AM improved survival in MCT rats without definite adverse effects.

PPH is a rare but life-threatening disease characterized by progressive pulmonary hypertension, ultimately producing right ventricular failure and death (25). Although intravenous administration of prostacyclin has become recognized as a therapeutic breakthrough (1, 6, 16, 26), some patients with PPH are refractory to this treatment. Thus a new therapeutic strategy for the treatment of PPH is desirable.

AM is one of the most potent endogenous vasodilators in the pulmonary vascular bed (5, 13, 14, 22). The vasodilating effect is mediated by a cAMP-dependent and/or nitric oxide-dependent mechanism (10, 20). Recently, we (19) have shown that intravenous administration of AM markedly decreases pulmonary vascular resistance in patients with PPH. Nevertheless, systemically administered AM decreases systemic arterial pressure, which may be harmful in treating patients with PPH. In the present study, inhalation of AM markedly decreased total pulmonary resistance, whereas it did not significantly decrease mean arterial pressure. The ratio of total pulmonary resistance to systemic vascular resistance was significantly reduced by AM inhalation. These results suggest that this novel route of AM administration causes relatively selective pulmonary vasodilation. Expectedly, inhalation of AM markedly increased the cardiac index in MCT rats, consistent with our previous results from intravenous delivery (18). Considering the strong vasodilator activity of AM in the pulmonary vasculature, the significant decrease in cardiac afterload may be responsible for the increased cardiac index with AM. Interestingly, the hemodynamic effects of AM lasted at least 60 min after a single inhalation of AM. Although a single inhalation of AM delivered 0.5 μg AM into the lungs in each rat, it induced only a slight increase in the plasma AM level (3.6 ± 1.0 fmol/ml). These results raise the possibility that inhaled AM is retained in lung tissue for a while and acts transepithelially on the pulmonary vasculature. Thus inhalation of AM may cause potent, long-lasting pulmonary vasodilator activity in MCT rats.

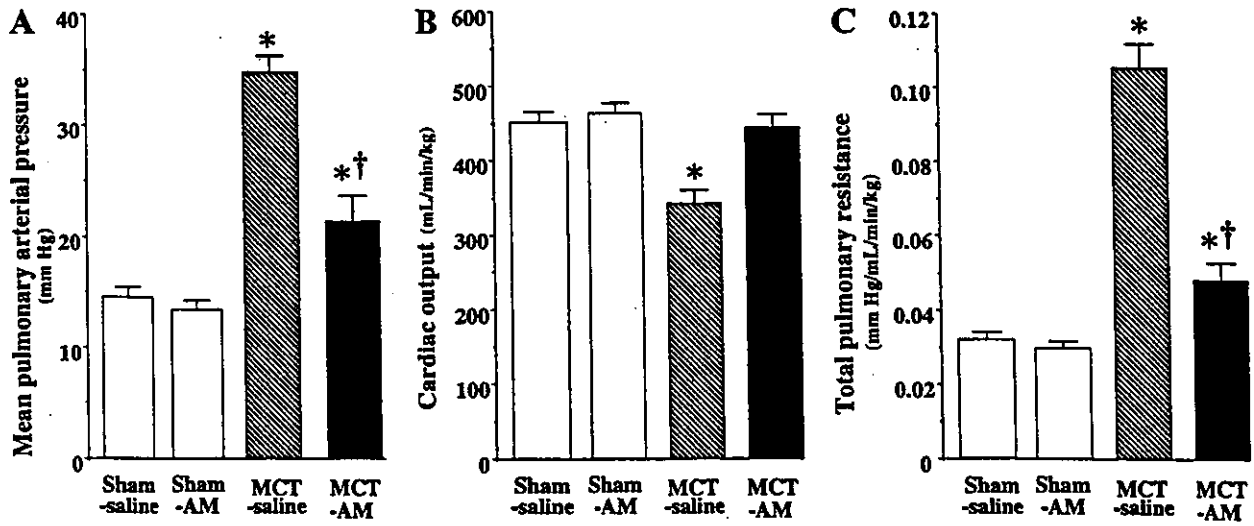

Fig. 2. Chronic effects of AM inhalation on mean pulmonary arterial pressure (*A*), cardiac output (*B*), and total pulmonary resistance (*C*). Sham-saline, sham rats given aerosolized AM; MCT-saline, MCT rats given aerosolized saline; sham-AM, sham rats given aerosolized AM; MCT-AM, MCT rats given aerosolized AM. Data are means ± SE. *$P < 0.05$ vs. sham-saline; †$P < 0.05$ vs. MCT-saline rats.